PHYSICAL REVIEW B VOLUME 39, NUMBER 16 1 JUNE 1989

Theory of the spin liquid state of the Heisenberg antiferromagnet

Vadim Kalmeyer
Department of Physics, Stanford University, Stanford, California 94305

R. B. Laughlin
Department of Physics, Stanford University, Stanford, California 94305
and Lawrence Livermore Laboratory, University of California, Livermore, California 94550
(Received 5 December 1988)

We propose that the disordered state of a two-dimensional spin-$\frac{1}{2}$ Heisenberg antiferromagnet is physically equivalent to the incompressible liquid state of the fractional quantum Hall system. The fractional quantum Hall state for bosons is shown to be an exact spin singlet and to possess a low variational energy for the near-neighbor Heisenberg model on a triangular lattice. Variational wave functions for neutral spin-$\frac{1}{2}$ excitations are constructed and shown to form an exact spin doublet. Variational energies of these states are calculated, and their spin density profiles are determined. We find that a localized spin-$\frac{1}{2}$ quaisparticle has a size comparable to a lattice bond length and an excitation energy $\Delta = 1.3J$. The energy-momentum dispersion of quasiparticles and spin-1 collective modes, obtained variationally, supports the hypothesis that the spin liquid state has a finite energy gap. The $\frac{1}{2}$ fractional statistics exhibited by the quasiparticle excitations is explicitly demonstrated.

I. INTRODUCTION

In a recent paper, we suggested[1] that the "resonating-valence-bond" (RVB) spin liquid state proposed by Anderson[2] to exist in frustrated Heisenberg antiferromagnets is physically equivalent to the fractional quantum Hall state. The purpose of this paper is to furnish some details supporting this idea and to report new results, including a proof that our ground state is a spin singlet and an estimate of energy dispersion of quasiparticles and collective modes.

The nature of the spin liquid state and its elementary excitations has recently been the subject of increasing interest in connection with the RVB theory of high-temperature superconductivity.[3] The properties of this state, and even its existence, are controversial. Anderson originally suggested[2] the near-neighbor Heisenberg model on a planar triangular lattice as a plausible candidate for the occurrence of a spin liquid. He constructed a disordered state for this Hamiltonian and found it to have a lower energy than the Néel state corrected for spin waves. The variational energy we reported[1] was essentially identical to Anderson's. Huse and Elser[4] subsequently constructed wave functions exhibiting long-range order which reportedly had a lower variational energy than either ours or Anderson's. This suggested that second-neighbor antiferromagnetic interactions were required to stabilize the liquid state. Recent results of Anderson, Liang, and Doucot[5] have demonstrated that the energy of variational wave functions for the Heisenberg model with near-neighbor coupling on a square lattice has an extremely weak dependence on the amount of Néel order inherent in the wave functions. In light of this controversy, exact solutions will probably be required to establish the existence and properties of the spin liquid state in a convincing way.[6]

Our theory[1] is based on the hypothesis that an adiabatic evolution of the fractional quantum Hall Hamiltonian into that of the antiferromagnet preserves the energy gap. Since the most important qualitative properties of the quantum Hall state, the incompressibility, nondegeneracy, and existence of fractionally charged particles, are associated with the presence of a gap,[7,8] this hypothesis is quite powerful. In particular, it implies that the ground state is a nondegenerate spin singlet with no translational long-range order, and that neutral spin-$\frac{1}{2}$ excitations must be present. These are the "spinons" proposed to occur in the RVB state.[9,10] Our identification resolves the conceptual problem posed by spin-$\frac{1}{2}$ excitations in a system like the Heisenberg antiferromagnet, where all basic degrees of freedom carry integer spin.

Since these properties of the spin liquid state follow necessarily from the adiabatic evolution hypothesis, it is incumbent on us to show that this hypothesis is reasonable. To do this, we shall show that the wave functions borrowed from the theory of the fractional quantum Hall effect provide a consistent description of the spin liquid. In particular, we shall show that the ground state is an exact spin singlet and a liquid, and that the variational energy of this state is competitive for the near-neighbor Heisenberg model on a triangular lattice. We shall also show that the collective mode wave function of Girvin, MacDonald, and Platzman[11] provides a sensible description of spin waves and that the quasiparticle wave functions form an exact spin doublet, as appropriate for spinons. The energy-momentum dispersion of spinons and collective modes, calculated from our variational basis, suggests that the energy gap is finite for all momentum-carrying excitations. Finally, we present numerical evi-

dence that spinons, described by quantum Hall wave functions on a lattice, obey fractional statistics.[12]

II. SPIN MODEL AS HARD-CORE BOSE GAS

We consider the spin-$\frac{1}{2}$ antiferromagnetic Heisenberg model with near-neighbor interactions on a two-dimensional triangular lattice as the prototype of a system possessing a spin liquid ground state. This choice of the model is reasonable,[2] but not essential: The adiabatic mapping procedure, discussed below, suggests that the spectrum of the system survives any change in the interaction Hamiltonian, as long as the system remains in the disordered phase. Our starting point is the Hamiltonian

$$\mathcal{H}=J\sum_{\langle ij\rangle}\mathbf{S}_i\cdot\mathbf{S}_j\ , \tag{2.1}$$

where $J>0$, $\mathbf{S}_j=\frac{1}{2}\boldsymbol{\sigma}_j$ is the spin operator at j^{th} lattice site, and the sum is over all sites i and, for each i, over its six near neighbors j. It is convenient to rewrite this Hamiltonian using the Holstein-Primakoff representation of the spin operators:

$$\begin{aligned} &S_j^+\rightarrow a_j^\dagger\ ,\\ &S_j^-\rightarrow a_j\ ,\\ &S_j^z\rightarrow a_j^\dagger a_j-\tfrac{1}{2}\ . \end{aligned} \tag{2.2}$$

The operator $a_j^\dagger$ creates a hard-core boson at j^{th} lattice site. Thus every spin state generates a configuration of the lattice bose gas where each up-spin site is occupied by a single boson and all down-spin sites are empty. We note that the triplet of operators (2.2) transforms according to the spin-1 representation of the spin algebra. The particle created by a_j thus carries spin equal to unity. The lattice gas Hamiltonian which follows from the Heisenberg interaction (2.1) is then

$$\mathcal{H}=T+V\ , \tag{2.3}$$

where

$$T=\frac{J}{2}\sum_{\langle ij\rangle}(a_j^\dagger a_i+a_i^\dagger a_j) \tag{2.3a}$$

describes near-neighbor hopping of bosons, and

$$V=J\sum_{\langle ij\rangle}a_i^\dagger a_i a_j^\dagger a_j-6J\sum_{i=1}^{N_s}a_i^\dagger a_i+\tfrac{3}{2}JN_s \tag{2.3b}$$

is, up to a constant, the potential energy of near-neighbor repulsion between bosons. N_s is the number of lattice sites. $\mathcal{H}$ also contains an implicit hard-core repulsion term

$$V_0=U_\infty\sum_{i=1}^{N_s}a_i^\dagger a_i^\dagger a_i a_i\ , \tag{2.3c}$$

which, in the limit $U_\infty\rightarrow\infty$, suppresses unphysical configurations with more than one boson on any site. This allows one to treat a_j and $a_j^\dagger$ as ordinary boson operators.

The term T can be identified as the kinetic energy of noninteracting charged particles moving on the lattice in the presence of a uniform "magnetic field" produced by the vector potential

$$\mathbf{A}(\mathbf{r})=\frac{B}{2}(x\hat{\mathbf{y}}-y\hat{\mathbf{x}})\ , \tag{2.4}$$

where the strength B of the magnetic field is chosen to produce exactly one-half of a flux quantum ϕ_0 per elementary plaquette of the lattice. The vector potential changes the phases of the single-boson hopping matrix elements according to

$$J_{ij}=-J\exp\left[\frac{2\pi i}{\phi_0}\int_i^j\mathbf{A}\cdot d\mathbf{l}\right]\ . \tag{2.5}$$

The matrix element $(-J)$ for free bosons in zero field is negative. Evaluating the phases induced by the magnetic field, we find

$$J_{ij}=JG(z_i)G(z_j)\ . \tag{2.6}$$

Here,

$$z_j=b\left[\left[l_j+\frac{1}{2}m_j\right]+i\frac{\sqrt{3}}{2}m_j\right]$$

is the complex coordinate for the j^{th} lattice site, l_j and m_j are integers, b is the bond length, and $G(z_j)$ is the gauge phase for the j^{th} site, given by

$$G(z_j)=(-1)^{l_j+m_j+l_jm_j+1}\ . \tag{2.7}$$

Thus, $G(z_j)$ is -1 on all lattice sites where $(l,m)=(\text{even},\text{even})$ and $+1$ on all other sites. Figure 1 shows the distribution of bond signs defined by Eqs. (2.6) and (2.7). This bond pattern differs from that appearing in T (all bonds positive) only by a local gauge transformation which reverses the sign of all single-boson orbitals at (even, even) sites, shown by solid circles in Fig. 1. The Hamiltonian (2.3) therefore describes a two-dimensional (2D) bose gas with near-neighbor repulsive interactions V, subject to a uniform magnetic field which represents

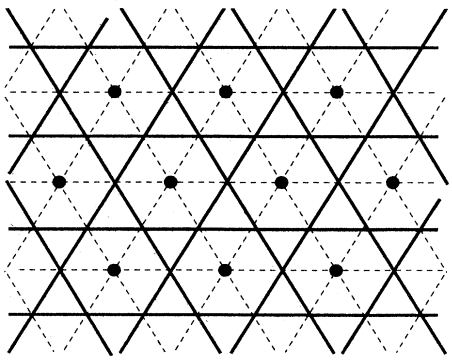

FIG. 1. Distribution of signs of the matrix elements defined by Eqs. (2.5) and (2.6). Solid lines, positive bonds; dashed lines, negative bonds. Solid circles denote sites where $G(z)=-1$.

the frustration inherent in the lattice.

The connection between the spin system and the fractional quantum Hall problem can now be established by the following thought experiment. Consider the *continuum* two-dimensional gas of charged bosons in a magnetic field. Now apply a periodic external potential which consists of a series of narrow wells centered on lattice sites, as shown in Fig. 2. One can then imagine slowly increasing the depth of these potential wells from zero to a point where all the bosons are effectively constrained to lattice sites. In the process the hopping matrix elements are kept constant and the range of the Coulomb repulsion is reduced to near-neighbor sites. One thus arrives at the lattice gas Hamiltonian (2.3). For the boson density corresponding to a half-filled lattice, the ground state of the initial continuum system is expected to be a nondegenerate liquid with an energy gap for elementary excitations.[7,8] The same properties then characterize the spin Hamiltonian (2.1), provided the lattice perturbation can be varied adiabatically and the energy gap remains finite as the continuum system is projected on the lattice.

In an equivalent realization of this adiabatic procedure, the fractional quantum Hall Hamiltonian is expressed in the complete basis of Gaussian orbitals,

$$\varphi_\alpha(z)=\frac{1}{\sqrt{2\pi}}e^{(-1/4)(|z|^2+|z_\alpha|^2)}e^{(1/2)z_\alpha^* z}, \tag{2.8}$$

where z_α is the coordinate of the α^{th} site. The continuum quantum Hall problem is then defined completely by the matrix elements of the Hamiltonian and the overlap matrix S:

$$S_{\alpha\beta}=\int d^2z\varphi_\alpha^*(z)\varphi_\beta(z) . \tag{2.9}$$

A continuum boson in the orbital φ_α has a nonzero probability to be also found in the orbital φ_β. Imposing the lattice constraint amounts to reducing the off-diagonal matrix elements of the overlap to zero.

This adiabatic mapping is almost certainly possible if the spin Hamiltonian has a spectrum with a finite energy gap. (We dismiss the unlikely possibility of a gap vanishing and then opening up again in the course of the time evolution, in which case the eigenstates of the spin and quantum Hall problems need not be related.) If the gap vanishes, the spectrum of the fractional quantum Hall Hamiltonian may still survive. Thus, fractional (spin-$\frac{1}{2}$) excitations exist in a one-dimensional (1D) Heisenberg chain[13] although the energy gap is zero in this system. A more probable result of the gap collapse is the onset of long-range antiferromagnetic order, analogous to Wigner crystallization in the quantum Hall system.[8,11] In what follows, we assume that the energy gap remains finite in the course of the evolution of the Hamiltonian, so the true ground state of the spin system (2.1) is a liquid.

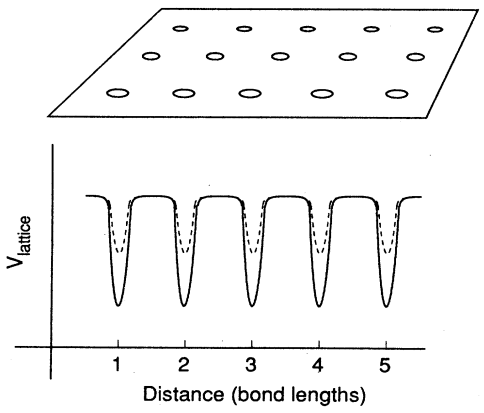

FIG. 2. Periodic external potential representing the lattice. As the depth of the potential wells increases, particles are confined to lattice sites.

III. GROUND-STATE PROPERTIES

We use the $m=2$ fractional quantum Hall wave function[7,8] to describe the ground state of the spin system. This choice leads to a liquid state which is a spin singlet and has a low variational energy. The wave function is

$$\Psi(z_1,\ldots,z_N)=\prod_{j<k}(z_j-z_k)^2\prod_{l=1}^{N}G(z_l)e^{(-1/4)|z_l|^2} . \tag{3.1}$$

Here, $z_j=x_j+iy_j$ is the complex coordinate of the lattice site occupied by j^{th} boson and N is the number of bosons. Since bosons mark the locations of up-spins in the lattice, $\Psi(z_1,\ldots,z_N)$ is the amplitude to find up-spins at sites $z_1,\ldots,z_N$ and down-spins at all other sites. The factor $G(z_l)$ is a gauge sign, defined in Eq. (2.7), which puts Ψ in the proper gauge where all hopping matrix elements in the term T of the Hamiltonian (2.3) are positive. All lengths are measured in units of the magnetic length $l_0=b(\sqrt{3}/4\pi)^{1/2}$, where b is the bond length.

The wave function (3.1) describes a lattice bose gas of uniform density $\rho=1/4\pi$. To verify this, note that the normalization sum for the ground state wave function (3.1) can be written as

$$Z\equiv\sum_{\{z_j\}}|\Psi(z_1,\ldots,z_N)|^2=\sum_{\{z_j\}}e^{-\beta\Phi(z_1,\ldots,z_N)} , \tag{3.2}$$

where $\beta=\frac{1}{2}$, each boson coordinate z_j, $j=1,\ldots,N$ is summed over the whole lattice, and

$$\Phi(z_1,\ldots,z_N)=-8\sum_{\langle ij\rangle}\ln|z_j-z_i|+\sum_{i=1}^{N}|z_i|^2 . \tag{3.3}$$

We identify Z as the partition function of a classical one-component lattice plasma. This plasma consists of N particles with "charge" 2 which move on lattice sites, interacting with each other via a repulsive Coulomb potential

$$v(z_j-z_i)=-4\ln|z_j-z_i| ,$$

as well as with a uniform neutralizing background of charge density $1/(2\pi)$. It will be shown below that this lattice plasma is a liquid, so the density of plasma particles is invariant under lattice translations. The density of bosons is thus uniform, i.e., the same on all lattice sites,

and is equal to $1/4\pi$, the background charge density divided by the fictive charge of the plasma particles, as required by plasma neutrality. In our system of units the unit cell area is $\Omega=2\pi$, so the average occupancy of any site is $\frac{1}{2}$. Translated into spin language, this means that each spin is equally likely to be either up or down, and the magnetization in the ground state is zero.

In order to show that the ground state (3.1) is a liquid, we calculate its two-spin correlation function,

$$c(i-j)\equiv\langle\Psi|\mathbf{S}_i\cdot\mathbf{S}_j|\Psi\rangle=3\langle\Psi|S_i^zS_j^z|\Psi\rangle\ .$$

The last equality follows from rotational invariance of the state $|\Psi\rangle$, proved below. Evaluating this in the lattice boson representation (2.2), we find

$$c(i-j)=\tfrac{3}{4}[g(i-j)-1]\ ,$$

for $i\neq j$, where $g(i-j)$ is the radial distribution function defined as

$$g(z_1-z_2)=\frac{4N(N-1)}{Z}\sum_{z_3}\cdots\sum_{z_N}|\Psi(z_1,z_2,\ldots,z_N)|^2\ , \tag{3.4}$$

Z is the normalization sum (3.2). The function $g(r)$ is the probability of finding two particles a distance r from each other, divided by the average occupancy of a site. We have computed $g(r)$ by a semiclassical Monte Carlo algorithm[8] and by a lattice generalization of the hypernetted chain (HNC) procedure which is described in Sec. V. The results of the two methods for the triangular lattice are compared in Table I and are plotted in Fig. 3. Beyond the third near-neighbor distance $r=2b$, $g(r)$ is within 0.3% of its asymptotic value of 1, indicating the absence of translational long-range order.

The decrease of $g(r)$ as $r\to 0$ is a direct effect of screening in the equivalent lattice plasma. Equation (3.4) indicates that $g(z_1-z_2)$ is proportional to the probability of finding two plasma particles at lattice sites z_1 and z_2. When $|z_1-z_2|\gg b$, the "charges" of the two particles are completely screened by the plasma, and this probability is a constant. As the particles are brought within a screening length of each other, screening becomes incomplete, and the Coulomb repulsion between the two particles reduces the probability of such configurations. The plasma analogy requires that the size of the screening hole in $g(r)$ satisfy two sum rules:

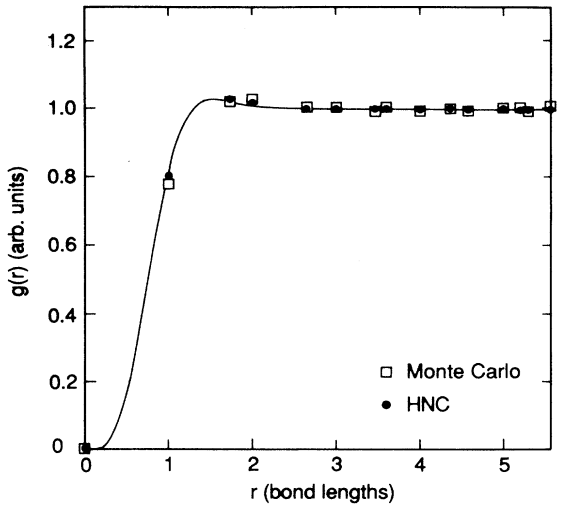

FIG. 3. Radial distribution function $g(r)$ in the ground state (3.1). The solid curve is an analytic fit to $g(r)$ defined by (6.14).

$$\sum_z[g(z)-1]=-2\ , \tag{3.5}$$

$$\sum_z|z|^2[g(z)-1]=-4\ . \tag{3.6}$$

Equation (3.5), known as the neutrality sum rule in continuum plasmas, states that the amount of "charge" missing from the screening hole is exactly equal to the "charge" of a plasma particle. Equation (3.6) is the constant-screening sum rule which follows from the $1/q^2$ divergence of the Coulomb potential in momentum space (cf. Sec. V). Both the Monte Carlo and the HNC results for $g(r)$ satisfy the two sum rules with 2% accuracy, i.e., within the error bars of the algorithms.

We now prove that the state (3.1) is a spin singlet. Although it is generally believed that the true ground state of the Heisenberg antiferromagnet is a singlet, this has only been shown[14] for unfrustrated systems. Our proof

TABLE I. Radial distribution function in the ground state (3.1), calculated by the Monte Carlo and HNC methods, and by the analytic fit formula (6.14).

r/b	Monte Carlo	HNC	Fit
0.0000	0.0000	0.0008	0.0000
1.0000	0.7773	0.8022	0.8020
1.7320	1.0210	1.0258	1.0225
2.0000	1.0273	1.0182	1.0094
2.6458	1.0052	0.9972	1.0002
3.0000	1.0030	0.9984	1.0000
3.4641	0.9904	1.0004	1.0000
3.6056	1.0049	1.0003	1.0000
4.0000	0.9941	1.0002	1.0000
4.3589	1.0012	1.0000	1.0000

depends crucially on the analyticity of the ground-state wave function Ψ and holds for both the triangular and the square lattices.

Since the wave function (3.1) is unmagnetized in the z direction, we need only prove that the total spin lowering operator $S_- = \sum_j S_j^-$ annihilates the ground state:

$$S_-|\Psi\rangle = 0 . \tag{3.7}$$

In the lattice boson language, the action of S_- gives a state of $(N-1)$ bosons, $|\Psi_-\rangle = \sum_j a_j|\Psi\rangle$, which is described in coordinate representation by the wave function

$$\sum_{z_1} \Psi(z_1, z_2, \ldots, z_N) .$$

This wave function is identically zero, as a consequence of the following theorem: if $F(z)$ is any polynomial, then

$$\sum_z G(z)F(z)\exp(-\tfrac{1}{4}|z|^2) = 0 , \tag{3.8}$$

where the sum is over all lattice sites and $G(z)$ is the gauge factor in the ground state (3.1). This theorem applies as well to the square lattice with unit cell area 2π, provided the gauge factors $G(z)$ are defined by (2.7) with $z_j = b(l_j + im_j)$.

An equivalent statement of theorem (3.8) is

$$\sum_z G(z) e^{(1/2)z_0^* z} e^{(-1/4)|z|^2} = 0 , \tag{3.9}$$

for every complex number z_0, since this series can be differentiated term by term. To establish (3.9), observe that

$$\sum_z G(z) e^{(1/2)z_0^* z} e^{(-1/4)|z|^2} = \sum_z e^{(1/2)z_0^* z} e^{(-1/4)|z|^2} - 2\sum_z e^{z_0^* z} e^{|z|^2} , \tag{3.10}$$

since the set of lattice vectors on which the gauge function $G(z)$ is negative is just the set of all lattice vectors multiplied by 2. We then evaluate the second sum in reciprocal space. The plane wave associated with any wave vector $\mathbf{G}$ may be written in the manner,

$$e^{-i\mathbf{G}\cdot\mathbf{r}} = e^{(\mathcal{G}z^* - \mathcal{G}^* z)/2} , \tag{3.11}$$

where $\mathcal{G} = G_y - iG_x$. Now if $\mathcal{G}$ is taken to represent a reciprocal lattice vector, then for any function $F(z)$,

$$\sum_z F(z) = \frac{1}{\Omega}\sum_{\mathcal{G}} \hat{\mathbf{F}}(\mathcal{G}) , \tag{3.12}$$

where $\hat{\mathbf{F}}(\mathcal{G})$ is the Fourier transform of $F(z)$, evaluated on the reciprocal lattice, and Ω is the unit cell size. Applying this to the last sum in (3.10), we find

$$\sum_z e^{z_0^* z} e^{|z|^2} = \frac{1}{2\pi}\sum_{\mathcal{G}} \int d^2\eta\, e^{z_0^*\eta} e^{-|\eta|^2} e^{(\mathcal{G}\eta^* - \mathcal{G}^*\eta)/2} = \tfrac{1}{2}\sum_{\mathcal{G}} e^{(\mathcal{G}/2)(z_0^* - \mathcal{G}^*/2)} . \tag{3.13}$$

In carrying out the integral, we have used the rule

$$\int d^2\eta F(\eta) e^{(-1/2m)|\eta|^2} e^{(1/2m)\eta^* z} = 2\pi m F(z) , \tag{3.14}$$

which holds for any polynomial $F(z)$. Now, because of our choice of the bond length for the direct lattice, the set of all $\mathcal{G}$'s is the same as the set of all direct lattice sites z. We then have

$$2\sum_z e^{z_0^* z} e^{|z|^2} = \sum_z e^{(1/2)z_0^* z} e^{(-1/4)|z|^2} , \tag{3.15}$$

which proves the theorem.

This proof reveals the special role of analytic wave functions in describing lattice spin systems. Evidently, any symmetric polynomial $F(z_1, z_2, \ldots, z_N)$ of continuum variables z_j, satisfying the hard-core constraint $F(z_1, z_1, \ldots, z_N) = 0$, yields a lattice spin state

$$\Psi(z_1, \ldots, z_N) = F(z_1, \ldots, z_N)\prod_{j=1}^{N} G(z_j)\exp(-\tfrac{1}{4}|z_j|^2) , \tag{3.16}$$

which is annihilated by S_-. If, furthermore, $S_z|\Psi\rangle = 0$, and if Ψ vanishes identically outside the sample boundary, then Ψ is a spin singlet state of the sample containing N_s spins. The singlet property of the liquid ground state (3.1) holds with exponentially high accuracy for $N_s \gg 1$.

These arguments remain fully intact if the wave function Ψ is replaced by its time reverse Ψ^*. We have thus constructed two disordered singlet states which are degenerate since the Heisenberg Hamiltonian is real. A direct calculation shows that the four-point correlation function in the ground state (3.1) is complex and, consequently, that the two states Ψ and Ψ^* are physically distinct. The four-point function is defined by

$$\chi_2(z_1', z_2' | z_1, z_2) = \frac{4N(N-1)}{Z}\sum_{z_3}\cdots\sum_{z_N} \Psi^*(z_1', z_2', z_3, \ldots, z_N)\Psi(z_1, z_2, z_3, \ldots, z_N) . \tag{3.17}$$

When z_1, z_1', z_2, and z_2' are triangular lattice sites, we find that χ_2 generally has a nonvanishing imaginary part such that $|\mathrm{Im}\ \chi_2|$ is maximized when $z_1 = z_1'$, z_2, and z_2' are vertices of an elementary plaquette. A Monte Carlo calculation yields

$$\mathrm{Im}\chi_2(0, b(\tfrac{1}{2} + i\sqrt{3}/2)|0, b) = 0.172 \pm 0.003 , \tag{3.18}$$

while an estimate based on analytic continuation of $g(z_1 - z_2)$ (as discussed in Sec. VI) gives $\mathrm{Im}\chi_2 = 0.15$ for the same set of arguments.

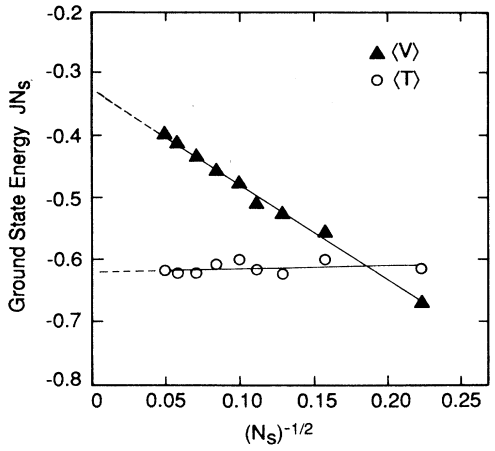

FIG. 4. Energy of the ground state (3.1) as a function of system size. Open circles: kinetic (XY) energy, triangles: potential (Ising) energy.

It is not clear at this point whether spontaneous breaking of time reversal symmetry is an essential property of the spin liquid phase. There is some indication that the liquid state of a spin-$\frac{1}{2}$ Heisenberg antiferromagnet on a two-dimensional square lattice has a discrete degeneracy.[15] If the time reversal symmetry is indeed broken by the true ground state, then excitations acquire a handedness which has an effect on their motion and statistics (cf. Secs. IX–XI).

The energy of the state (3.1) has been calculated by the Monte Carlo method for lattices of up to 400 sites. We work with the lattice gas Hamiltonian (2.3) and use free boundary conditions. The wave function (3.1) confines the particles to a circular droplet of radius proportional to $N_s^{1/2}$. The potential energy per site therefore has a boundary contribution which scales like $N_s^{-1/2}$. The extrapolation to the thermodynamic limit is well defined, as shown in Fig. 4, and yields the following ground-state energy expectation values:

$$\langle T\rangle/JN_s=-0.62\pm0.02\ ,$$

$$\langle V\rangle/JN_s=-0.32\pm0.01\ .$$

Since $\langle T\rangle$ and $\langle V\rangle$ arise, respectively, from the XY and Ising terms in the Heisenberg Hamiltonian, the virial relation $\langle T\rangle=2\langle V\rangle$ is consistent with spin-rotational invariance of the singlet state Ψ. The total energy $E=-0.94\pm0.02$ is compared in Table II with other ground-state energy estimates for the triangular lattice antiferromagnet.[2,4,16] The energy of our state is surprisingly low, given the absence of any variational freedom.

IV. SPIN INVERSION SYMMETRY

The ground-state wave function has been taken to depend on the coordinates of up-spins. The same amplitude can equally well be considered a function of the down-spin locations $\eta_1,\ldots,\eta_N$:

$$\bar{\Psi}(\eta_1,\ldots,\eta_N)\equiv\Psi(z_1,\ldots,z_N)\ . \tag{4.1}$$

We now show explicitly that $\bar{\Psi}$ has the same functional form as Ψ, up to a phase which is constant is the thermodynamic limit

$$\Psi(z_1,\ldots,z_N)=\bar{\Psi}(z_1,\ldots,z_N)e^{i\theta}\ . \tag{4.2}$$

In the boson language, this is a statement of particle-hole symmetry of the ground state: the amplitude to find bosons on a given set of sites is the same, up to a global phase, as the amplitude to find holes (empty sites) at the same locations. This symmetry is a special case of the rotational invariance of the ground state established in the previous section. The independent proof given here serves as a cross check of the singlet sum rule (3.8) and the product rule (4.3) below, both of which will be used in later sections.

The proof makes use of the following theorem:

$$\prod_{j\neq k}(\zeta_k-\zeta_j)=C_0G(\zeta_k)\exp(\tfrac{1}{4}|\zeta_k|^2)\ , \tag{4.3}$$

where ζ_j are lattice sites, $G(\zeta_k)$ are the gauge signs (cf. Sec. II), and C_0 is constant in the thermodynamic limit. To prove (4.3), we define the following function of a continuous complex variable ζ:

$$f_k(\zeta)=\prod_{j\neq k}^{N_s}(\zeta-\zeta_j)\ . \tag{4.4}$$

We are interested in the behavior of this function as $\zeta\to\zeta_k$. Taking the logarithm of (4.4), we get

$$\ln f_k(\zeta)=R(\zeta)+\Delta R_k(\zeta)+i\Phi_k(\zeta)\ , \tag{4.5a}$$

where

$$R(\zeta)=\sum_{j=1}^{N_s}\ln|\zeta-\zeta_j|\ , \tag{4.5b}$$

$$\Delta R_k(\zeta)=-\ln|\zeta-\zeta_k|\ , \tag{4.5c}$$

$$\Phi_k(\zeta)=\arg[f_k(\zeta)]\ . \tag{4.5d}$$

The term $R(\zeta)$ can be interpreted as the two-dimensional

TABLE II. Estimates of the ground-state energy for the near-neighbor Heisenberg antiferromagnet on the triangular lattice.

Exact diagonalization of small clusters (Ref. 16)	-1.09 ± 0.02
Three-parameter variational wave functions (Ref. 4)	-1.07
Near-neighbor RVB state (Ref. 2)	-0.95
This work	-0.94 ± 0.02

Coulomb energy of a particle of charge $-\frac{1}{2}$ located at ζ and interacting with a system of fixed unit charges at lattice sites ζ_j. Isolating the energy due to the average charge density $1/2\pi$, we write,

$$R(\zeta)=\tfrac{1}{4}|\zeta|^2-\sum_{\mathcal{G}\neq 0}\frac{1}{|\mathcal{G}|^2}e^{(1/2)(\mathcal{G}\zeta^*-\mathcal{G}^*\zeta)} . \tag{4.6}$$

When ζ approaches a lattice site, the exponentials in (4.6) all tend to unity, and the sum diverges logarithmically. For the special case $\zeta\rightarrow\zeta_k$, this logarithmic divergence is offset by the divergence in $\Delta R_k(\zeta)$, so their sum R_0 is independent of ζ_k unless ζ_k is very close to the sample boundary. Thus,

$$R(\zeta)+\Delta R_k(\zeta)\xrightarrow[\zeta\rightarrow\zeta_k]{}\tfrac{1}{4}|\zeta_k|^2+R_0 . \tag{4.7}$$

The remaining task is to calculate the phase $\Phi_k(\zeta)$. Consider the phase change

$$\Delta\Phi_{kk'}\equiv\Phi_{k'}(\zeta_{k'})-\Phi_k(\zeta_k) ,$$

where ζ_k and $\zeta_{k'}$ are near neighbors, and let ζ_{mid} be any point along the bond kk'. Then, (4.5d) implies

$$\Phi_{k'}(\zeta_{\text{mid}})-\Phi_k(\zeta_{\text{mid}})=\pi , \tag{4.8}$$

and, using the definition of $\Delta\Phi_{kk'}$, we obtain

$$\Delta\Phi_{kk'}=\pi+\int_{\zeta_k}^{\zeta_{\text{mid}}}\nabla\Phi_k\cdot d\mathbf{r}+\int_{\zeta_{\text{mid}}}^{\zeta_{k'}}\nabla\Phi_{k'}\cdot d\mathbf{r} . \tag{4.9}$$

Since the function $\ln[f_k(\zeta)]$ is differentiable at $\zeta=\zeta_k$, its real and imaginary parts satisfy the Cauchy-Riemann equations

$$\begin{aligned}\frac{\partial}{\partial x}[R(\zeta)+\Delta R_k(\zeta)]&=\frac{\partial}{\partial y}\Phi_k(\zeta) ,\\ \frac{\partial}{\partial y}[R(\zeta)+\Delta R_k(\zeta)]&=-\frac{\partial}{\partial x}\Phi_k(\zeta) ,\end{aligned} \tag{4.10}$$

where $x+iy=\zeta$. These equations allow one to replace the gradient of the phase along the bond kk' by the derivative of $R(\zeta)+\Delta R_k(\zeta)$ normal to the bond. Evaluated along the line kk', this normal derivative vanishes by reflection symmetry about kk' for all terms in $R(\zeta)+\Delta R_k(\zeta)$ except for the uniform background potential $\frac{1}{4}|\zeta|^2$. Differentiation of this term gives

$$\begin{aligned}\Delta\Phi_{kk'}&=\pi+\int_{\zeta_k}^{\zeta_{k'}}(-\tfrac{1}{2}ydx+\tfrac{1}{2}xdy)\\ &=\pi+\frac{1}{B}\int_{\zeta_k}^{\zeta_{k'}}\mathbf{A}(\mathbf{r})\cdot d\mathbf{r} ,\end{aligned} \tag{4.11}$$

where

$$\mathbf{A}(\mathbf{r})=\frac{B}{2}(-y\hat{\mathbf{x}}+x\hat{\mathbf{y}})$$

is precisely the vector potential which changes the signs of all bonds when combined with the gauge transformation $G(z)$, as follows from Eqs. (2.5) and (2.6). Therefore,

$$e^{i\Delta\Phi_{kk'}}=G(\zeta_{k'})G(\zeta_k) . \tag{4.12}$$

Combining (4.7) and (4.12), we obtain the product rule (4.3).

If the lattice is finite, both $R(\zeta)$ and $\Phi_k(\zeta)$ contain boundary terms. The finite-size correction to $R(\zeta)$, for example, is the two-dimensional Coulomb potential produced by a zero-average "lattice charge" distribution restricted to the exterior of the sample. Such corrections are essentially higher multipole fields which are guaranteed to be negligible for all ζ inside the sample.

Eqn. (4.3) can be used to rewrite the ground-state wave function (3.1) as follows:

$$\Psi(z_1,\ldots,z_N)=\prod_{j\neq k}(z_j-z_k)^2\left[\prod_{\alpha,k}{}'(\zeta_\alpha-z_k)\right]^{-1}C_0^N . \tag{4.13}$$

Here, ζ_α runs over all lattice sites while the z's are locations of bosons. The prime on the second product excludes the terms $\zeta_\alpha=z_k$. If $\{\eta_1,\ldots,\eta_N\}$ is the corresponding set of unoccupied site coordinates, then we may write

$$\prod_{\alpha,k}{}'(\zeta_\alpha-z_k)=\prod_{j\neq k}(z_j-z_k)\prod_{\alpha,n}(\eta_\alpha-z_n) , \tag{4.14}$$

and (4.13) takes the simple form,

$$\Psi(z_1,\ldots,z_N)=-\left[\prod_{\alpha,n}(\eta_\alpha-z_n)\right]^{-1}C_0^N . \tag{4.15}$$

Inversion symmetry of the ground state is now manifest since interchanging z_n and η_α in (4.15) gives only a global sign change. The amplitude for a given spin configuration to occur in the ground state is thus equal to the amplitude of its spin-flipped image.

V. THE HYPERNETTED CHAIN PROCEDURE

The hypernetted chain algorithm[17] is an approximate method of calculating the radial distribution function $g(r)$ [cf. Eq. (3.4)] of a classical liquid with short-range pair interactions $v(r)$. If the particles of the liquid are confined to a lattice, we write the HNC equations as

$$h(r_j)=g(r_j)-1 , \tag{5.1}$$

$$g(r_j)=\exp[-\beta v(r_j)-c(r_j)+h(r_j)] , \tag{5.2}$$

$$h(r_j)=c(r_j)+\rho\Omega\sum_k c(\mathbf{r}_j-\mathbf{r}_k)h(\mathbf{r}_k) , \tag{5.3}$$

where Ω is the unit cell area, ρ is the particle density per unit area, β^{-1} is the temperature, and the sum is over all lattice sites. The approximation step in the continuum version of the HNC equations involves setting to zero a "bridge function" in the exponential of Eq. (5.2). The bridge function, which must be included to obtain the exact $g(r)$, is known to be small and short ranged for the continuum liquid.[17] Restricting the HNC equations to the lattice has an unknown effect on the bridge function; thus, the validity of the lattice HNC procedure rests on comparison of the results with Monte Carlo calculations.

We use Eqs. (5.1)–(5.3) to calculate $g(r)$ for the lattice plasma defined by the probability distribution in the ground state (3.1). As discussed in Sec. III, this plasma is characterized by the temperature $\beta^{-1}=2$ and the

Coulomb pair potential

$$\beta v(r) = -4\ln(r) .$$

Since this potential is *long-ranged,* the lattice HNC equations must be regularized in order to be computationally stable. This is done in a manner analogous to the continuum plasma calculation.[8] For a liquid, the function $h(r_j)$ is short-ranged; therefore, in the limit $r_j \to \infty$, the logarithm in $-\beta v_s(r_j)$ must be cancelled by a long-range term in $c(r_j)$, as indicated by Eqs. (5.1) and (5.2). To make use of this cancellation, we define the *short-ranged* potential v_s and function c_s:

$$\beta v_s(r_j) = \frac{2}{\pi}\int \frac{e^{i\mathbf{q}\cdot\mathbf{r}_j}}{q_0^2+q^2} d^2q = 4K_0(q_0 r_j) , \tag{5.4}$$

$$c_s(r_j) = c(r_j) + \frac{2}{\pi}\int \frac{Q^2 e^{i\mathbf{q}\cdot\mathbf{r}_j}}{q^2(q^2+Q^2)} d^2q . \tag{5.5}$$

Here, q_0 is the fictive inverse "screening length", Q is an arbitrary cutoff momentum whose value is chosen to improve convergence, and K_0 is a modified Bessel function. In the limit $q_0 \to 0$, the potential v_s reduces to the Coulomb form:

$$\beta v_s(r_j) \to -4\ln(q_0 r_j/2) .$$

Hence, we have

$$\beta v(r_j) + c(r_j) = c_s(r_j) + \frac{2}{\pi}\int \frac{e^{i\mathbf{q}\cdot\mathbf{r}_j}}{q^2+Q^2} d^2q , \tag{5.6}$$

and Eq. (5.2) assumes the following regularized form:

$$g(r_j) = \exp[h(r_j) - c_s(r_j) - 4K_0(Qr_j)] . \tag{5.7}$$

The coupled equations (5.1), (5.3), (5.5), and (5.7) can be solved iteratively by introducing the Fourier transforms

$$\hat{h}(q) = 2\pi \sum_j h(r_j) e^{-i\mathbf{q}\cdot\mathbf{r}_j} , \tag{5.8}$$

$$\hat{c}_s(q) = 2\pi \sum_j c_s(r_j) e^{-i\mathbf{q}\cdot\mathbf{r}_j} , \tag{5.9}$$

$$\hat{c}(q) = \hat{c}_s(q) - 8\pi \sum_{\mathbf{G}} \frac{Q^2}{[(\mathbf{q}+\mathbf{G})^2+Q^2](\mathbf{q}+\mathbf{G})^2} , \tag{5.10}$$

where $\mathbf{q}$ lies in the Brillouin zone and $\mathbf{G}$ runs over the reciprocal lattice. Equation (5.3) then becomes

$$\hat{h}(q) = \frac{\hat{c}(q)}{1 - \frac{1}{4\pi}\hat{c}(q)} , \tag{5.11}$$

since $\rho = 1/4\pi$ and $\Omega = 2\pi$. Having chosen the value of the cutoff momentum Q, we use the following iteration scheme to compute $g(r_j)$ numerically. First, the function $c_s(r_j)$ is initialized to zero. Then, Eq. (5.9) is used to Fourier transform $c_s^{\text{old}}(r_j)$ which is known either from initialization or from the previous iteration. The function $\hat{h}^{\text{new}}(q)$ is then obtained from (5.10) and (5.11), back transformed into $h^{\text{new}}(r_j)$, and compared with $[g^{\text{new}}(r_j) - 1]$ calculated from (5.7). The function $c_s(r_j)$ is then updated according to

$$c^{\text{new}}(r_j) = c^{\text{old}}(r_j) + g^{\text{new}}(r_j) - 1 - h^{\text{new}}(r_j) . \tag{5.12}$$

With $Q = 2b^{-1}$, this procedure converges to 0.1% level in 16 iterations.

The radial distribution function calculated by the lattice HNC procedure agrees with $g(r)$ calculated by the Monte Carlo method within 5%, the largest discrepancy being in the near-neighbor value $g(b)$ (see Fig. 3 and Table I). Figure 5 shows the Fourier transforms $\hat{c}_s(q)$ and $\hat{h}(q)$, used in the HNC calculation of $g(r)$, for $\mathbf{q}$ along the line from the center to the corner of the Brillouin zone. Since the Coulomb divergence has been extracted from $\hat{c}_s(q)$, this function is finite in the limit $q \to 0$. Although $\hat{c}_s(q)$ depends strongly on the choice of the cutoff momentum Q, the converged results for $\hat{h}(q)$ and $g(r)$ are independent of Q in the range $1 \le bQ \le 4$.

The origin of the constant screening sum rule for $g(r)$, Eq. (3.6), can now be clarified. This sum rule follows by observing that the function $h(r_j)$ is always short-ranged in a liquid. Hence, no matter what the approximate short range form of Eq. (5.2) is, in the limit $r_j \to \infty$ the Coulomb potential must be *exactly* cancelled by the logarithmic divergence in $c(r_j)$. The exact $g(r_j)$ can thus be represented by the Ornstein-Zernike equation (5.11) where

$$\hat{c}(q) \to \hat{c}_0 - \frac{8\pi}{q^2} , \tag{5.13}$$

in the limit $q \to 0$. Equation (5.11) then implies

$$\hat{h}(q) \to 4\pi(-1 + \tfrac{1}{2}q^2) , \tag{5.14}$$

and the sum rule (3.6) follows immediately:

$$\sum_j r_j^2 h(r_j) = -\lim_{q\to 0} \nabla_q^2 \left[\frac{1}{2\pi}\hat{h}(q)\right] = -4 . \tag{5.15}$$

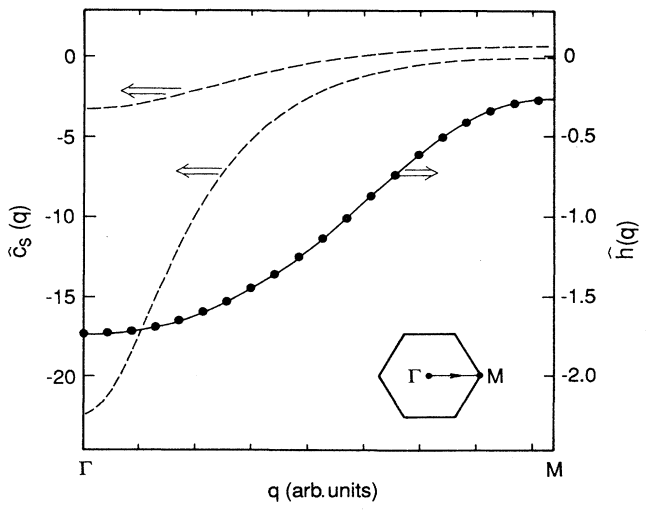

FIG. 5. Fourier transforms $\hat{h}(q)$ and $\hat{c}_s(q)$ vs q along the line ΓM in the Brillouin zone (inset). Dashed lines: $\hat{c}_s(q)$ for $bQ = 2$ and $bQ = 1$ (upper and lower curves). $\hat{h}(q)$ is shown by circles for $bQ = 1$, and by a solid line for $bQ = 2$.

Both sum rules (3.5) and (3.6) are satisfied within 2% by the correlation function calculated using the HNC procedure.

VI. ANALYTIC CONTINUATION OF CORRELATION FUNCTIONS

The noninvariance of the spin liquid state Ψ under time reversal, as discussed in Sec. III, is evidenced by the behavior of the correlation functions in this state. In particular, Monte Carlo calculations indicate that the four-point function $\chi_2(z_1',z_2'|z_1,z_2)$ defined by (3.17) has a nonzero imaginary part. We now verify this result by an independent method which makes use of the analytic properties of the ground-state wave function (3.1).

As a test of the analytic continuation technique, we first prove that the two-point correlation function (the density matrix) in the ground state, defined by

$$\chi(z_1'|z_1)=\frac{1}{Z}\sum_{z_2}\cdots\sum_{z_N}\Psi^*(z_1',z_2,\ldots,z_N)\Psi(z_1,z_2,\ldots,z_N)\ . \tag{6.1}$$

is *real* when z_1 and z_1' are lattice sites. This is expected to be true because the wave function Ψ is invariant under global spin rotations: setting the normalization Z to unity, we may write, for $z_j\neq z_i$,

$$\begin{aligned}\chi(z_j|z_i)&=\langle\Psi|S_j^+S_i^-|\Psi\rangle=2\langle\Psi|S_j^zS_i^z|\Psi\rangle\\&=\tfrac{1}{2}[g(z_j-z_i)-1]\ ,\end{aligned} \tag{6.2}$$

where $g(z)$ is the (real) radial distribution function defined by Eq. (3.4). An independent proof of the reality of $\chi(z_1'|z_1)$ uses the fact that

$$G(z_1)\exp(\tfrac{1}{4}|z_1|^2)\Psi(z_1,\ldots,z_N)$$

is an *analytic* function of z_1. Ignoring the irrelevant gauge signs $G(z)$, χ, therefore, has the form

$$\chi(z_1'|z_1)=\exp[-\tfrac{1}{4}(|z_1'|^2+|z_1|^2)]\sum_{m,n}c_{m,n}(z_1'^*)^n(z_1)^m\ . \tag{6.3}$$

The coefficients $c_{m,n}$ and thus the whole function $\chi(z_1'|z_1)$ may be deduced from $\chi(z_1|z_1)$ if it is known for *all* values of z_1, including those not associated with lattice sites. There is a simple algorithm for achieving this analytic continuation of χ: if the value of the function

$$F(z)=\sum_{m,n}c_{m,n}(z^*)^n(z)^m \tag{6.4}$$

is known for all z, then we can evaluate

$$c_{m,n}=\frac{1}{2\pi(m+n)!}\left[\frac{\partial}{\partial r}\right]_{r=0}^{m+n}\int d\theta F(re^{i\theta})e^{i(n-m)\theta}\ . \tag{6.5}$$

In the present case, $\chi(z_1|z_1)$ is just a constant times the "probability" to find one of the particles at z_1. This must be a periodic function since all sites are physically equivalent, and thus we may write

$$\chi(z_1|z_1)=\sum_{\mathcal{G}}a_{\mathcal{G}}\exp[\tfrac{1}{2}(\mathcal{G}z_1^*-\mathcal{G}^*z_1)]\ , \tag{6.6}$$

where $\mathcal{G}$ is a complex reciprocal lattice vector [cf. Eq. (3.11)] and $a_{\mathcal{G}}$ is a real number, as required by the reality of $\chi(z_1|z_1)$ and the inversion symmetry of the lattice. Analytically continuing this, we obtain

$$\chi(z_1'|z_1)=\exp[-\tfrac{1}{4}(|z_1'|^2+|z_1|^2)]\exp(\tfrac{1}{2}z_1'^*z_1)\sum_{\mathcal{G}}a_{\mathcal{G}}\exp[\tfrac{1}{2}(\mathcal{G}z_1'^*-\mathcal{G}^*z_1)]\ . \tag{6.7}$$

We now constrain z_1 and z_1' to be lattice vectors. The imaginary part of the argument of the $\mathcal{G}=0$ exponential is then

$$\begin{aligned}\mathrm{Im}(\tfrac{1}{2}z_1'z_1)&=\tfrac{1}{2}b^2\,\mathrm{Im}\{[j'+(\tfrac{1}{2}+i\sqrt{3}/2)k'][j+(\tfrac{1}{2}-i\sqrt{3}/2)k]\}\\&=\frac{4\pi}{\sqrt{3}}\frac{\sqrt{3}}{2}(jk'-j'k)=\pi(jk'-j'k)\ .\end{aligned} \tag{6.8}$$

This exponential is therefore real. However, since the set of all $\mathcal{G}$'s is the same as the set of all lattice vectors z, the exponential factors are real for every value of $\mathcal{G}$. This, together with the reality of $a_{\mathcal{G}}$, shows that $\chi(z_1'|z_1)$ is real.

The Fourier components $a_{\mathcal{G}}$ have been calculated by Monte Carlo and are found to decrease rapidly with $|\mathcal{G}|$. The "density" profile $\chi(z_1|z_1)$ across the unit cell is thus nearly constant, with most of the variation arising from the first shell of $\mathcal{G}$ vectors. The Monte Carlo results for the coefficients $a_{\mathcal{G}}$ are compared in Table III with the values obtained

by inverting the equation

$$e^{(-1/4)|z|^2}\sum_{\mathcal{G}} a_{\mathcal{G}} e^{(1/2)\mathcal{G}z^*}=\tfrac{1}{2}[g(z)-1]\ , \tag{6.9}$$

which follows from (6.2) and (6.7). The analytically continued form (6.7) of the two-point function $\chi(z_1'|z_1)$ is seen to be consistent with rotational invariance of the ground state.

The same analytic continuation argument can be used to obtain an approximate formula for the four-point correlation function

$$\chi_2(z_1',z_2'|z_1,z_2)=\frac{4N(N-1)}{Z}\sum_{z_3}\cdots\sum_{z_N}\Psi^*(z_1',z_2',z_3,\ldots,z_N)\Psi(z_1,z_2,z_3,\ldots,z_N)\ . \tag{6.10}$$

and to estimate its imaginary part. When $z_1'=z_1$ and $z_2'=z_2$, χ_2 is equal to the radial distribution function $g(z_1-z_2)$ of the classical plasma. Thus, if z_1 and z_2 are lattice sites, $\chi_2(z_1,z_2|z_1,z_2)$ quickly approaches unity as $|z_1-z_2|$ becomes larger than a bond length b (see Fig. 3). For any z_1 and z_2 we therefore have

$$\chi_2(z_1,z_2|z_1,z_2)=\text{const}\,\chi(z_1|z_1)\chi(z_2|z_2)+\delta\chi_2(z_1,z_2|z_1,z_2)\ , \tag{6.11}$$

where $\delta\chi_2$ is a function that is negligibly small unless $|z_1-z_2|\le b$. Since the continuation of $\chi(z_1'|z_1)$ away from $z_1'=z_1$ is already known, the task is to analytically continue $\delta\chi_2$. From the Bose symmetry of the ground-state wave function, $\chi_2(z_1',z_2'|z_1,z_2)$ must be symmetric under interchange $z_1\leftrightarrow z_2$ or $z_1'\leftrightarrow z_2'$. The analytic continuation of $\delta\chi_2(z_1,z_2|z_1,z_2)$ must therefore have the form

$$\delta\chi_2(z_1',z_2'|z_1,z_2)=\text{const}\,\chi(z_1'|z_2)\chi(z_2'|z_1)+\delta f(z_1',z_2'|z_1,z_2)\ . \tag{6.12}$$

The remaining term $\delta f(z_1',z_2'|z_1,z_2)$ must be (i) analytic in z_1, z_2, $z_1'^*$, and $z_2'^*$, except for the familiar Gaussian factors, (ii) a periodic function in the center-of-mass coordinates $(z_1+z_2)/2$, $(z_1'+z_2')/2$, and (iii) a short-range function of the difference coordinates $|z_1-z_2|$, $|z_1'-z_2'|$, etc. These conditions are satisfied by the following parametrization of δf:

$$\delta f=\exp[-\tfrac{1}{4}(|z_1'|^2+|z_2'|^2+|z_1|^2+|z_2|^2)]\exp[\tfrac{1}{4}(z_1+z_2)(z_1'^*+z_2'^*)]\sum_{n=0}^{\infty}b_n[(z_1-z_2)^2(z_1'^*-z_2'^*)^2]^n\ , \tag{6.13}$$

where b_n are arbitrary coefficients.

The representation of $\chi_2(z_1',z_2'|z_1,z_2)$, defined by Eqs. (6.11)–(6.13), should reduce to $g(z_1-z_2)$ when $z_1=z_1'$ and $z_2=z_2'$. If we now approximate the "density profile" $\chi(z|z)$ within the unit cell by a constant by setting all Fourier coefficients $a_{\mathcal{G}}$ in (6.6) except for a_0 to zero, we obtain the following expression for the radial distribution function:

$$g(z_1-z_2)=C\left[1+e^{(-1/2)|z_1-z_2|^2}+e^{(-1/4)|z_1-z_2|^2}\sum_n b_n|z_1-z_2|^{4n}\right]\ . \tag{6.14}$$

This form of $g(r)$ can now be used to fit the coefficients b_n and thus to determine χ_2 analytically. Setting b_3, $b_4,\ldots=0$, the parameters C, b_0, b_1, and b_2 are uniquely defined by the limiting behavior of $g(r)$,

$$\lim_{r\to 0}g(r)=0\ ,\qquad \lim_{r\to\infty}g(r)=1\ , \tag{6.15}$$

and by the two plasma sum rules (3.5) and (3.6), whereby $C=1$, $b_0=-2$, $b_1=0.0114$, and $b_2=8\times10^{-6}$. With this choice of parameters, the approximate form (6.14) of $g(r)$ gives the fit to the radial distribution function shown by the solid line in Fig. 3.

TABLE III. Fourier coefficients $a_{\mathcal{G}}$ of the density function $\chi(z_1|z_1)$. $\mathcal{G}$ is a reciprocal lattice vector, and $a_0\equiv1$ by normalization. HNC values of $g(r)$ shown in Table I have been used in Eq. (6.9). The error bars on the Monte Carlo values are of order ±0.04.

$\lvert\mathcal{G}\rvert/b$	Monte Carlo	Eq. (6.9)
0.0000	1.00	1.00
1.0000	0.13	0.12
1.7320	0.04	0.00
2.0000	0.05	0.00
2.6458	0.06	0.00

The imaginary part of χ_2 comes entirely from the short-ranged term (6.13). The maximum of $\mathrm{Im}\chi_2$ is attained when $z_1=z_1'$, z_2, and z_2' are the vertices of an elementary triangular plaquette. Explicit evaluation of expression (6.13) gives

$$\mathrm{Im}\chi_2(0,b(1/2+i\sqrt{3}/2)|0,b)=0.151\ , \tag{6.16}$$

while the Monte Carlo value is

$$\mathrm{Im}\chi_2=0.172\pm.003$$

for the same set of arguments. The magnitude of this imaginary part is a measure of how far the ground-state wave function Ψ is from being equivalent to its time reverse.

VII. SPIN-$\frac{1}{2}$ QUASIPARTICLE EXCITATIONS

It is an experimental fact that fractionally charged elementary excitations exist in quantum Hall samples.[7,8,18] Their existence is consistent with the fractional quantization of the Hall conductance[18] and follows necessarily from the nondegeneracy of the quantum Hall ground state and the presence of an energy gap in the excitation spectrum. To review the reasoning leading to this conclusion,[7,8] consider the quantum Hall system of electrons in the ground state with uniform density $\rho_m = 1/(2\pi m)$ where m is an odd integer. Now insert a thin solenoid (flux tube) at the origin and slowly thread the magnetic flux through it. When one quantum of flux ϕ_0 has been injected, the vector potential produced by the solenoid is a pure gauge, so the system Hamiltonian is unaffected by the presence of the extra flux. Since low-energy excitations are absent, the evolution of the system is adiabatic and results in an exact eigenstate of the quantum Hall Hamiltonian. This eigenstate is an excitation, since work has been done on the system. The charge carried by this quasiparticle excitation can be determined by noting that threading one flux quantum through the solenoid shifts the lowest Landau level states over by one. This is shown schematically in Fig. 6(a), where the lowest Landau level eigenstate

$$\psi_{k,0}(z) = z^k \exp[(-1/4)|z|^2]$$

in the symmetric gauge is represented by a thin annulus with mean radius

$$\langle \psi_{k,0} | r^2 | \psi_{k,0} \rangle^{1/2} \simeq \sqrt{2k}\,, \quad \text{for } k \gg 1\,.$$

The charge of the quasiparticle excitation is thus equal to the ground-state charge per state in a Landau level, or e/m, where e is the electron charge.

Similar fractionally charged excitations are expected to occur in the continuum 2D gas of charge e hard-core bosons, provided a nondegenerate liquid state with an energy gap exists in this system. If the density of this gas is $1/(4\pi)$, corresponding to the $m = 2$ quantum Hall ground state, quasiparticle excitations have charge $e/2$. What happens to these fractionally charged quasiparticles as the continuum system is projected on the lattice? Suppose the liquid state with a nonzero energy gap survives on the lattice. One can then imagine a sample where the strength of the external potential confining the particles to lattice sites is slowly reduced with radial distance from the center, and is zero beyond some large radius R, as shown in Fig. 6(b) where the strength of the lattice potential is indicated by the size of the dots. A flux tube is now placed at the origin (in the lattice region), and the flux-winding experiment of the previous paragraph is repeated. Although the behavior of the bose gas near the flux tube is unknown, the amount of charge crossing a circular boundary of any radius $r > R$ lying in the continuum region is certain to be $e/2$. Since the energy gap is assumed to be finite *everywhere* in the sample, the ground-state charge distribution slides rigidly, except near the flux tube. This region of the lattice thus contains a quasiparticle excitation of the lattice gas, carrying a total charge exactly equal to $e/2$.

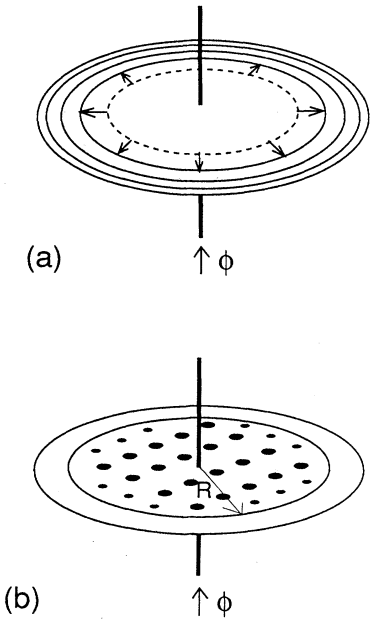

FIG. 6. (a) The flux-injection experiment for the continuum quantum Hall system. The annular "tracks" represent lowest Landau level eigenstates. (b) A similar experiment for the lattice system smoothly connected to a continuum sample. The size of the dots is proportional to the strength of the confining lattice potential.

In terms of spin degrees of freedom, a quasiparticle with charge $e/2$ represents a neutral spin-$\frac{1}{2}$ excitation of the antiferromagnet. This follows from the fact that creating a lattice boson with charge e is tantamount to flipping a single spin, which increases the total S_z by one unit of $\hbar$. These spin-$\frac{1}{2}$ quasiparticles should exist as excitations of the spin Hamiltonian as long as the system ground state is a liquid with a finite-energy gap. The spin of the quasiparticle is *exactly* $\frac{1}{2}$, as follows from the flux-winding argument given above. The finite energy required to create a quasiparticle can be interpreted as the self-energy of formation of the charge cloud in the equivalent lattice gas. For a rotationally invariant Hamiltonian, the quasiparticle and its spin-reversed state, the quasihole, are degenerate and should be viewed as two polarization states of a spin-$\frac{1}{2}$ particle.

Such neutral spin-$\frac{1}{2}$ excitations are known as *spinons* in the context of the RVB state.[9,10] Their existence appears to be a generic feature of the liquid state in spin-$\frac{1}{2}$ magnets.[12] The visible lack of trial wave functions for the spinon indicates that combining spin-1 objects in a coherent quantum state with total spin $\frac{1}{2}$ is a difficult task. Since this is exactly what the fractional quantum Hall wave

functions do, we use them as a variational basis for describing spinons. A spin-down spinon localized at the point z_0 is represented by the quasihole wave function[7,8]

$$\Psi^{\downarrow}_{z_0}(z_1,\ldots,z_N)=S^{\downarrow}_{z_0}\Psi(z_1,\ldots,z_N)\ , \tag{7.1}$$

where Ψ is the ground state (3.1) and $S^{\downarrow}_{z_0}$ is the quasihole creation operator

$$S^{\downarrow}_{z_0}=\prod_{i=1}^{N}(z_i-z_0)\ . \tag{7.2}$$

The action of the operator $S^{\downarrow}_{z_0}$ is to push the lattice bosons away from the quasihole center z_0, which produces a dip in the up-spin density near z_0. The spin-up quasiparticle is the spin-flip image of the quasihole: we obtain its wave function from Eqs. (7.1) and (7.2) by replacing boson coordinates $\{z_1,\ldots,z_N\}$ by empty site coordinates $\{\eta_1,\ldots,\eta_N\}$:

$$\Psi^{\uparrow}_{z_0}(z_1,\ldots,z_N)=S^{\uparrow}_{z_0}\Psi(z_1,\ldots,z_N)\ . \tag{7.3}$$

where the quasiparticle creation operator $S^{\uparrow}_{z_0}$ is defined as

$$S^{\uparrow}_{z_0}=\prod_{i=1}^{N}(\eta_i-z_0)\ . \tag{7.4}$$

Here the product is over all empty site coordinates corresponding to the occupied site configuration $\{z_1,\ldots,z_N\}$. The ground-state wave function Ψ is unaffected by the interchange $z\leftrightarrow\eta$ because of its spin inversion symmetry (cf. Sec. IV).

These wave functions have the correct spin-rotation properties expected of spin-$\frac{1}{2}$ particles: $\Psi^{\uparrow}_{z_0}$ and $\Psi^{\downarrow}_{z_0}$ transform as components of a spin doublet. Since the wave function (7.1) is analytic in the up-spin coordinates, Eq. (3.8) implies

$$S_-\Psi^{\downarrow}_{z_0}=0\ . \tag{7.5}$$

One can also show that S_- converts a quasiparticle into a quasihole

$$S_-\Psi^{\uparrow}_{z_0}=\text{const}\,\psi^{\downarrow}_{z_0}\ . \tag{7.6}$$

It suffices to prove (7.6) when z_0 is a lattice site, since any quasiparticle wave function can be written as a linear combination of such states (cf. Sec. IX). In the lattice boson representation, the state vector representing a quasiparticle localized at z_0 is

$$|\Psi^{\uparrow}_{z_0}\rangle=\sum_{z_1}\cdots\sum_{z_N}\Psi^{\uparrow}_{z_0}(z_1,\ldots,z_N)a^{\dagger}_{z_1}\cdots a^{\dagger}_{z_N}|0\rangle\ , \tag{7.7}$$

where the vacuum $|0\rangle$ is the state with no bosons. For every finite sample with N bosons in the state $|\Psi^{\uparrow}_{z_0}\rangle$, the action of the total spin lowering operator S_- produces a state with $(N-1)$ bosons, described by the wave function

$$\Psi_-=\sum_{z'}\Psi^{\uparrow}_{z_0}(z',z_1,\ldots,z_{N-1})\ , \tag{7.8}$$

where the sum is over all sites z'. We now observe that, up to a normalization, Ψ_- is identical to $\Psi^{\downarrow}_{z_0}(z_1,\ldots,z_{N-1})$. First, examine the term $z'=z_0$ in (7.8). Using the product rule (4.3), we have

$$\begin{aligned}\Psi^{\uparrow}_{z_0}(z_0,z_1,\ldots,z_{N-1})&=\left[\prod_{\alpha}(\eta_\alpha-z_0)\prod_{i=1}^{N-1}(z_i-z_0)^2G(z_0)e^{-(1/4)|z_0|^2}\right]\prod_{j<k}(z_j-z_k)^2\prod_{l=1}^{N-1}G(z_l)e^{-(1/4)|z_l|^2}\\&=C\Psi^{\downarrow}_{z_0}(z_1,\ldots,z_{N-1})\ ,\end{aligned} \tag{7.9}$$

where C is a constant in the thermodynamic limit. The remaining terms in (7.8) can be shown to sum to zero, as follows. When $z'\neq z_0$, the amplitude $\Psi^{\uparrow}_{z_0}(z',z_1,\ldots,z_{N-1})$ vanishes unless the quasiparticle center z_0 is occupied by one of $(N-1)$ bosons, say the jth one. Since $\Psi^{\uparrow}_{z_0}$ is symmetric under interchange of boson coordinates, we can repeat the arguments leading to (7.9) to get

$$\begin{aligned}\Psi^{\uparrow}_{z_0}(z',z_1,\ldots,z_j,\ldots,z_{N-1})&=\Psi^{\uparrow}_{z_0}(z_0,z_1,\ldots,z',\ldots,z_{N-1})\\&=C\Psi^{\downarrow}_{z_0}(z_1,\ldots,z',\ldots,z_{N-1})\ .\end{aligned} \tag{7.10}$$

The right-hand side of (7.10) is explicitly of the form $G(z')\,F(z')e^{-(1/4)|z'|^2}$, where $F(z')$ is a polynomial in z'. The "singlet" sum rule (3.8) is thus applicable and gives

$$\sum_{z'\neq z_0}\Psi^{\uparrow}_{z_0}(z',z_1,\ldots,z_{N-1})=C\sum_{z'}\Psi^{\downarrow}_{z_0}(z_1,\ldots,z',\ldots,z_{N-1})=0\ , \tag{7.11}$$

which proves (7.6). The states $|\Psi_{z_0}^{\uparrow}\rangle$ and $|\Psi_{z_0}^{\downarrow}\rangle$ thus transform into each other under spin rotations like two components of an $s=\frac{1}{2}$ spinor.

VIII. EXCITATION ENERGY AND SPIN DENSITY PROFILE OF A SPINON

The wave functions (7.1)–(7.4) can be used to calculate the spinon excitation energy variationally. Before doing this, we point out that rotation properties of the quasihole and quasiparticle states lead to a generally valid "virial" relation between the contributions of the terms T and V in the Hamiltonian (2.3) to the total energy of a spinon. We have

$$\langle s|T|s\rangle = 2\langle s|V|s\rangle \ , \tag{8.1}$$

where $|s\rangle$ is a spinon state with $S_z=s$. The same relation holds for the T and V values in the singlet ground state (3.1), as discussed in Sec. III. Without loss of generality, we prove (8.1) for the quasiparticle state $|\uparrow\rangle$. Since the term T follows from the XY part of the Heisenberg interaction, invariance of $|\uparrow\rangle$ under rotations about the z axis implies

$$\langle\uparrow|T|\uparrow\rangle = 2J\left\langle\uparrow\left|\sum_{\langle ij\rangle} S_i^x S_j^x\right|\uparrow\right\rangle \ . \tag{8.2}$$

Let R_y be the operator for a global spin rotation by $\pi/2$ about the y axis:

$$R_y = e^{(-i\pi/2)S_y} \ . \tag{8.3}$$

where $S_y=\sum_j S_j^y$. The spinon state $|\uparrow\rangle$ is polarized in the z direction. Under the action of R_y, it is oriented along the x axis:

$$R_y|\uparrow\rangle = \frac{1}{\sqrt{2}}(|\uparrow\rangle+|\downarrow\rangle) \ , \tag{8.4}$$

while the xx interaction transforms into

$$JR_y\left[\sum_{\langle ij\rangle} S_j^x S_i^x\right]R_y^{-1} = J\sum_{\langle ij\rangle} S_j^z S_i^z = V \ . \tag{8.5}$$

Thus, (8.2) implies

$$\langle\uparrow|T|\uparrow\rangle = (\langle\uparrow|+\langle\downarrow|)V(|\uparrow\rangle+|\downarrow\rangle) \ . \tag{8.6}$$

Since V conserves S_z, the cross terms in (8.6) vanish while the remaining terms are equal, which proves the virial relation (8.1).

The excitation energy for a localized spinon described by Eqs. (7.1)–(7.4) has been calculated by the Monte Carlo and HNC methods, as discussed below. The Monte Carlo results for the T and V contributions to the spinon creation energy Δ_s are shown as discrete points in Fig. 7 for lattices of various sizes (up to $N_s=300$). The dashed lines in Fig. 7 represent the HNC value $\Delta V^{\rm HNC}=0.42J$ and the prediction $\Delta T^{\rm HNC}=0.84J$ which follows from (8.1). These numerical results are consistent with the virial relation (8.1) and yield the total excitation energy $\Delta_s=3\Delta V=1.26J$ for a spinon localized on a lattice site. (The previously reported estimate[1] of Δ_s was incorrect.)

The Monte Carlo calculation of the spinon energy Δ_s

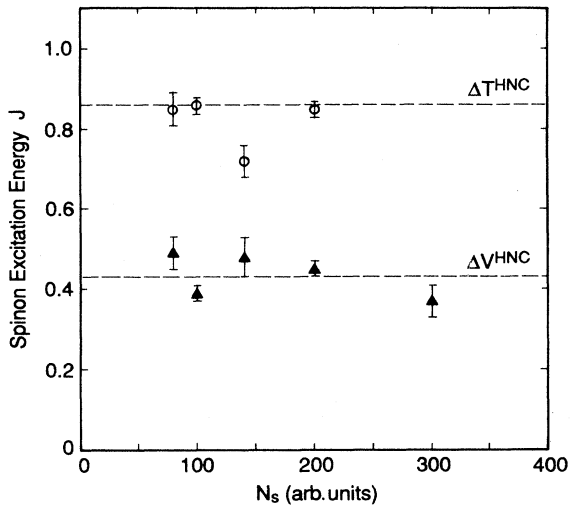

FIG. 7. Excitation energy for a spinon localized on a lattice site. Dashed lines are drawn at HNC values; points are Monte Carlo data. Triangles: potential energy; circles: kinetic energy.

was carried out for the state $|z_A\downarrow,z_B\uparrow\rangle$ containing a quasihole at site z_A and a quasiparticle at z_B, where $|z_A-z_B|=4b$. The addition of a second spinon with opposite polarization makes the total S_z zero; the region of the lattice occupied by bosons is therefore the same in the state $|z_A\downarrow,z_B\uparrow\rangle$ and in the ground state $|\Psi\rangle$. This causes the boundary effects (which scale as $N_s^{-1/2}$ for V, as Fig. 4 indicates) to disappear from Δ_s which is obtained as follows:

$$\Delta_s = \tfrac{1}{2}(\langle z_A\downarrow,z_B\uparrow|\mathcal{H}|z_A\downarrow,z_B\uparrow\rangle - \langle\Psi|\mathcal{H}|\Psi\rangle) \ . \tag{8.7}$$

This expression is valid if the two spinons are separated by a distance z_A-z_B large on the scale of the plasma screening length, and are thus independent (see discussion below). When $|z_A-z_B|\geq 3b$, we find the left-hand side of (8.7) to be unchanged as we vary the separation distance.

The energy and correlation functions in the localized spinon state have also been calculated using a generalization of the HNC method described in Sec. V. The generalized HNC procedure for the quasihole localized at z_0 derives from the partition function

$$\langle\Psi_{z_0}^{\downarrow}|\Psi_{z_0}^{\downarrow}\rangle e^{(-1/4)|z_0|^2} = \sum_{z_1}\cdots\sum_{z_N} e^{-\beta\Phi'(z_0,z_1,\ldots,z_N)} \ , \tag{8.8}$$

where

$$\beta\Phi' = \tfrac{1}{4}|z_0|^2 - 2\sum_{i=1}^{N}\ln|z_i-z_0| - 4\sum_{j<k}\ln|z_j-z_k| + \tfrac{1}{2}\sum_{l=1}^{N}|z_l|^2 \tag{8.9}$$

is the Coulomb potential energy of a lattice plasma consisting of N particles with "charge" 2 interacting with a neutralizing background and with a "phantom" particle

of "charge" 1, fixed at z_0. If the phantom is allowed to move on the lattice, it will be found on any site with equal probability, The plasma is thus a mixture of two interpenetrating liquids: one made up of type-one particles with charge 2 and uniform density $\rho_1=1/(4\pi)$; the other consisting of type-two particles (phantoms) with charge 1 and density $\rho_2=1/(4\pi N)$.

The two correlation functions of interest are $g_{11}(z_1-z_2)$, which measures the probability to find two type-1 particles separated by a distance z_1-z_2, and $g_{12}(z_1-z_0)$, which gives the probability to find a type-1 particle a distance z_1-z_0 from the phantom. These are calculated using the two-component HNC equations[8]

$$h_{ab}(r_j)=g_{ab}(r_j)-1\ , \tag{8.10}$$

$$g_{ab}(r_j)=\exp[-\beta v_{ab}(r_j)+h_{ab}(r_j)-c_{ab}(r_j)]\ , \tag{8.11}$$

$$h_{ab}(r_j)=c_{ab}(r_j) +\Omega\sum_c \rho_c \sum_k h_{ac}(\mathbf{r}_j-\mathbf{r}_k)c_{cb}(r_k)\ . \tag{8.12}$$

Here, a, b, and c run over the two types of particles, $\mathbf{r}_j$ and $\mathbf{r}_k$ run over lattice sites, $v_{ab}(r)$ is the Coulomb potential energy of particles of type a and b separated by r, and $\Omega=2\pi$ is the unit cell area. These coupled equations can be solved perturbatively,[8,19] as described below, by expanding in the small parameter ρ_2.

The function $h_{12}(r)$ is equal to the twice the average spin at r due to a quasihole centered at the origin. This spin density profile is plotted in Fig. 8 as a function of r. The quasihole wave function (7.1) forces the spin at the origin to be down; hence, $h_{12}(0)=-1$, as expected. Apart from this dip at the quasihole center, the spin density is close zero. One can therefore think of the quasihole (quasiparticle) creation operator as simply fixing the spin at z_0 to be down (up). The rest of the spin liquid then adjusts to this, but because of the short plasma screening length the change in the local spin density away from z_0 is small.

The potential energy required to create a localized quasihole is obtained by noting that the presence of the quasihole also changes the radial distribution function by a small amount $\delta g_{11}(r)$ of order $1/N$, relative to $g(r)$ in the ground state. The near-neighbor value $\delta g_{11}(b)$ yields the potential energy ΔV required to create a localized quasihole:

$$\Delta V=3JN\delta g_{11}(b)\ . \tag{8.13}$$

The HNC calculation gives $N\delta g_{11}(b)=0.14$, whence $\Delta V^{\rm HNC}=0.42J$, as shown in Fig. 7. Since $\delta g_{11}\sim 1/N$, ΔV is a constant independent of N in the thermodynamic limit.

The finiteness of Δ_s is an indication that the liquid ground state remains incompressible on the lattice. However, a complete variational estimate of the energy gap should take into account the energy-momentum dispersion of moving quasiparticles and collective excitations. These will be discussed in Secs. IX and X.

We now review the perturbative solution[8,19] of the two-component HNC equations which yields the correlation functions $g_{11}(r)$ and $g_{12}(r)$. The approach is first to solve Eqs. (8.10)–(8.12) with ρ_2 set to zero, then to linearize (8.11) and (8.12) in all quantities of order $\mathcal{O}(\rho_2)$ and compute the correlations $h_{11}(r)$ and $h_{12}(r)$ to that order. The first step involves regularizing Eq. (8.11) along the lines of Sec. V, which gives

$$g_{1a}^{(0)}(r_j)=\exp[h_{1a}^{(0)}(r_j)-c_{s_{1a}}^{(0)}(r_j)-2m_aK_0(Qr_j)] \tag{8.14}$$

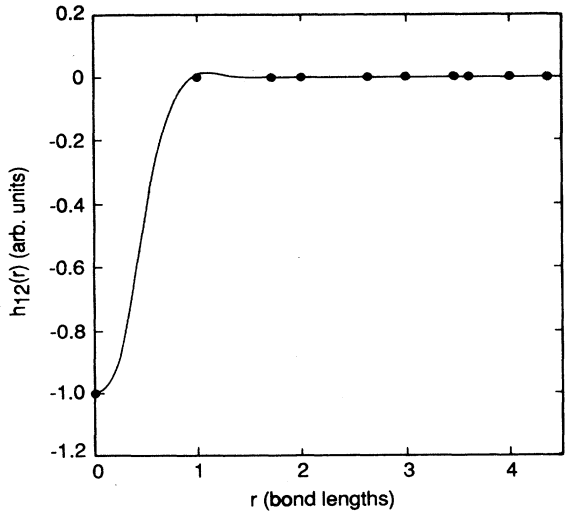

FIG. 8. Spin distribution around a quasihole localized at the origin. Circles are values calculated by the two-component HNC procedure. The solid curve is a guide to the eye.

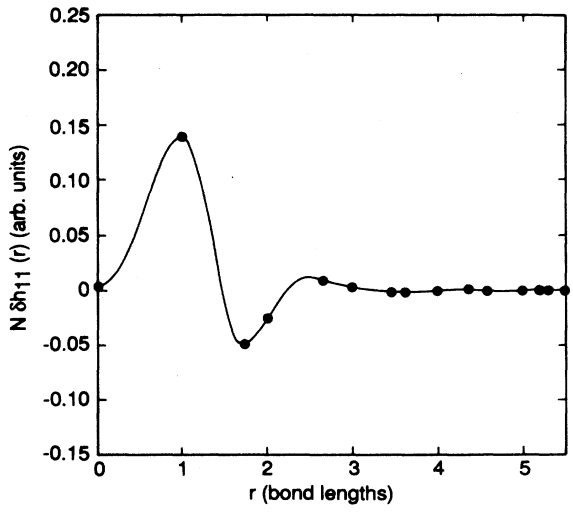

FIG. 9. Change in the radial distribution function due to the presence of a quasihole excitation. Circles are values of $N\delta h_{11}(r)$ obtained by the two-component HNC method. Solid curve is a guide to the eye.

where $m_1=2$ and $m_2=1$ are the plasma "charges" of type-1 and type-2 particles, respectively, and the superscript indicates 0th order of perturbation theory in ρ_2. In terms of the Fourier transforms, defined by Eqs. (5.8)–(5.9), the short-range c functions are given by

$$\hat{c}^{(0)}_{s_{1a}}(q)=\hat{c}^{(0)}_{1a}(q)-\sum_G \frac{4\pi m_a Q^2}{[(\mathbf{q}+\mathbf{G})^2+Q^2](\mathbf{q}+\mathbf{G})^2} , \quad (8.15)$$

where the sum on G is over the reciprocal lattice. The Ornstein-Zernike equation (8.12) with $\rho_2=0$ is

$$\hat{h}^{(0)}_{1a}(q)=\frac{\hat{c}^{(0)}_{1a}(q)}{1-\rho_1\hat{c}^{(0)}_{1a}(q)} . \quad (8.16)$$

Having solved Eqs. (8.10) and (8.14)–(8.16) for $a=1,2$ iteratively, as discussed in Sec. V, the second step consists of expanding Eqs. (8.11) and (8.12) to first order in all quantities of $O(1/N)$. Besides $\rho_2=1/(4\pi N)$, these include the small corrections δc_{1a}, δh_{1a}, $a=1,2$ caused by the presence of the type-2 particle. The correction δh_{12}, a small change in the spin density distribution around the quasihole, vanishes in the thermodynamic limit and is irrelevant. The quantity of interest is $\delta h_{11}=\delta g_{11}$, since it determines the quasihole energy, according to (8.13). Linearizing Eq. (8.11) for g_{11}, we find

$$\delta g_{11}(r_j)=[\delta h_{11}(r_j)-\delta c_{11}(r_j)]g^{(0)}_{11}(r_j) , \quad (8.17)$$

or, in view of (8.10),

$$\delta h_{11}(r_j)=\delta c_{11}(r_j)\{1+[h^{(0)}_{11}(r_j)]^{-1}\} . \quad (8.18)$$

An expansion of Eq. (8.12), expressed in Fourier space, yields

$$\delta\hat{h}_{11}(q)=\delta\hat{c}_{11}(q)+\rho_1[\delta\hat{h}_{11}(q)\hat{c}^{(0)}_{11}(q)+\hat{h}^{(0)}_{11}(q)\delta\hat{c}_{11}(q)]+\rho_2\hat{h}^{(0)}_{12}(q)\hat{c}^{(0)}_{12}(q) , \quad (8.19)$$

which is combined with (8.16) to give

$$\delta\hat{h}_{11}=\delta\hat{c}_{11}(1+\rho_1\hat{h}^{(0)}_{11})^2+\rho_2(\hat{h}^{(0)}_{11})^2 . \quad (8.20)$$

The pair of linear equations (8.18) and (8.20) are finally solved for δh_{11} and δc_{11} with the 0th order quantities $h^{(0)}_{11}$ and $h^{(0)}_{12}$ entering as input from the first step. In Fig. 9 we show the solution $\delta h_{11}(r_j)$ which gives the correction to the ground state $g(r_j)$ due to the presence of the quasihole. For the near-neighbor separation b, we find $\delta g_{11}(b)=\delta h_{11}(b)=0.14$ in units of $1/N$. This leads to the value of the quasihole energy given above.

IX. ITINERANT QUASIPARTICLE STATES

For a translationally invariant Hamiltonian, the spin-$\frac{1}{2}$ eigenstates can be described by extended wave functions in a complete basis of states. We choose this basis to be the set of all localized spinon orbitals of the form

$$|z_0,\alpha\rangle=e^{(-1/8)|z_0|^2}S^{\alpha}_{z_0}|\Psi\rangle , \quad (9.1)$$

where $\alpha=\uparrow,\downarrow$ is the spin index, z_0 is the center of the spinon, and the operators $S^{\alpha}_{z_0}$ are defined by (7.2) and (7.4). If z_0 is allowed to range over all lattice sites, this basis is twice overcomplete, as we shall demonstrate below. Our goal is to construct extended spinon states

$$|k,\alpha\rangle=\sum_{z_0}\psi_k(z_0)|z_0,\alpha\rangle , \quad (9.2)$$

labeled by a crystal momentum k. We note, however, that the basis of localized orbitals (9.1) is nonorthogonal, so the itinerant state (9.2) must satisfy a Schrodinger equation of the form

$$(\mathcal{H}-E_kS)\psi_k=0 , \quad (9.3)$$

where

$$S_{ij}=\langle z_j,\alpha|z_i,\alpha\rangle$$

is the overlap matrix and

$$\mathcal{H}_{ij}=\langle z_j,\alpha|\mathcal{H}|z_i,\alpha\rangle$$

is the Hamiltonian projected on the spinon subspace (9.1). Since the Hamiltonian has the translation symmetry of the lattice, the matrices $\mathcal{H}$ and S have the same set of eigenvectors. The energy E_k is therefore given by the ratio of the eigenvalues of $\mathcal{H}$ and S corresponding to the common eigenvector ψ_k.

The overlap matrix for the localized spinon states may be found using the analytic continuation technique developed in Sec. VI to analyze the ground-state density matrix. The overlap matrix $\langle z'_0,\beta|z_0,\alpha\rangle$ is diagonal in the spin indices α and β and is a periodic function of z_0 when $z'_0=z_0$. The latter follows from the plasma partition function (8.8) and (8.9). The definition of the spinon operators implies that the quantity $\langle\Psi|(S^{\alpha}_{z'_0})^{\dagger}(S^{\alpha}_{z_0})|\Psi\rangle$ is analytic in z'^{*}_0 and z_0. Repeating the arguments of Sec. VI, we obtain the following analytic continuation of the overlap matrix for all z'_0,z_0:

$$\langle z'_0,\beta|z_0,\alpha\rangle=\delta_{\alpha\beta}\exp[-\tfrac{1}{8}(|z'_0|^2+|z_0|^2)]\exp(\tfrac{1}{4}z'^{*}_0z_0)\sum_{\mathcal{G}}A_{\mathcal{G}}\exp[\tfrac{1}{2}(\mathcal{G}z'^{*}_0-\mathcal{G}^{*}z_0)] , \quad (9.4)$$

where $\mathcal{G}$ are the complex reciprocal lattice vectors and $A_{\mathcal{G}}$ are real coefficients. The matrix elements of the Hamiltonian $\mathcal{H}$ have the same analytic structure as the overlap matrix, since $\mathcal{H}$ acts only on the boson degrees of freedom. Therefore, $\langle z'_0,\beta|\mathcal{H}|z_0,\alpha\rangle$ has the form (9.4) with $A_{\mathcal{G}}$ replaced by the real Fourier coefficients $B_{\mathcal{G}}$ defined by

$$\langle z_0,\alpha|\mathcal{H}|z_0,\alpha\rangle=\sum_{\mathcal{G}} B_{\mathcal{G}}\exp[\tfrac{1}{2}(\mathcal{G}z_0^*-\mathcal{G}^*z_0)]\ , \tag{9.5}$$

where z_0 is allowed to vary throughout the unit cell of the lattice.

We can now write down the solutions of the Schrodinger equation (9.3). These spinon states have the form

$$|Q,\Delta,\alpha\rangle=\sum_{z_A}{}'\exp\{\tfrac{1}{2}[Q^*(z_A+\Delta)-Q(z_A^*+\Delta^*)]\}|z_A+\Delta,\alpha\rangle\ . \tag{9.6}$$

Here the sum is over sites on the "even" sublattice $z_A=2z$, as indicated by the prime. The state $|Q,\Delta,\alpha\rangle$ is a plane wave superposition of spinons localized in Gaussian orbitals centered at points $(z_A+\Delta)$, as shown in Fig. 10. The wave vector $Q=Q_y-iQ_x$, the displacement $\Delta=\Delta_x+i\Delta_y$, and the spin index α are the quantum numbers characterizing the moving spinon. To prove that the state (9.6) is a solution of (9.3), consider the action of the overlap matrix on this state. Using (9.4), we find

$$\langle z_0',\alpha|Q,\Delta,\alpha\rangle=\lambda_{Q-\Delta/4}\sum_{z_A}{}'\exp[\tfrac{1}{8}(|z_0|^2+|z_A+\Delta|^2)]\exp[\tfrac{1}{4}z_0^*(z_A+\Delta)]\exp\{\tfrac{1}{2}[Q^*(z_A+\Delta)-Q(z_A^*+\Delta^*)]\}\ , \tag{9.7}$$

where z_0 is any complex number and $\lambda_{Q-\Delta/4}$ is defined by

$$\lambda_k=\sum_{\mathcal{G}} A_{\mathcal{G}}e^{k\mathcal{G}^*-k^*\mathcal{G}}e^{1/2|\mathcal{G}|^2}\ . \tag{9.8}$$

Since the Hamiltonian matrix differs from the overlap matrix only by its Fourier components $B_{\mathcal{G}}$, the action of $\mathcal{H}$ on $|Q,\Delta,\alpha\rangle$ follows trivially:

$$\langle z_0',\alpha|\mathcal{H}|Q,\Delta,\alpha\rangle=\frac{\varepsilon_{Q-\Delta/4}}{\lambda_{Q-\Delta/4}}\langle z_0',\alpha|Q,\Delta,\alpha\rangle\ , \tag{9.9}$$

where $\varepsilon_{Q-\Delta/4}$ is given by (9.8) with $A_{\mathcal{G}}$ replaced by $B_{\mathcal{G}}$. This proves that $|Q,\Delta,\alpha\rangle$ is an eigenstate of $\mathcal{H}$ with energy $E_k=\varepsilon_k/\lambda_k$, where $k=Q-\Delta/4$.

We identify the quantity $k=Q-\Delta/4$ as the crystal momentum associated with the state $|Q,\Delta,\alpha\rangle$. This identification is confirmed by the fact that states with different k's are orthogonal: using the eigenvalue equation (9.7), we find

$$\langle Q',\Delta',\alpha|Q,\Delta,\alpha\rangle=\delta_{k,k'}\lambda_k M_k(\Delta,\Delta')\ , \tag{9.10}$$

where $k=Q-\Delta/4$, $k'=Q'-\Delta'/4$, and

$$M_k(\Delta,\Delta')=e^{(-1/8)|\Delta-\Delta'|^2}e^{1/8(\Delta'^*\Delta-\Delta'\Delta^*)}e^{1/2[k(\Delta'^*-\Delta^*)-k^*(\Delta'-\Delta)]}\sum_z e^{(-1/2)|z|^2}e^{zk^*-z^*k}e^{1/2(z\Delta'^*-z^*\Delta)}\ . \tag{9.11}$$

Furthermore, as expected of a crystal momentum, the quantum number k is conserved in neutron-spinon scattering. If the momentum transfer is q, the matrix element for a neutron to scatter a spinon from the state $|Q,\Delta,\alpha\rangle$ into the state $|Q',\Delta',\alpha\rangle$ is zero unless

$$(Q-\Delta/4)-(Q'-\Delta'/4)=q\ .$$

Within each subspace $(\alpha,k=\text{const})$, there are exactly two independent states. This is verified numerically by computing the determinant of the matrix $M_k(\Delta,\Delta')$; for any three states with the same k, this determinant is zero. There are therefore two degenerate spinon bands for each polarization state α, which we label $|k,\Delta_1,\alpha\rangle$ and $|k,\Delta_2,\alpha\rangle$. Although we have not done so, the eigenvectors of M_k can be used to construct the two orthogonal states for each (k,α).

The overlap of localized spinon orbitals reduces the range of crystal momenta by "folding" the lattice Brillouin zone. Equation (9.6) implies that states $|Q,\Delta,\alpha\rangle$ and $|Q',\Delta,\alpha\rangle$ with $Q'-Q=G/2$, where G is a reciprocal lattice vector, are linearly dependent. The crystal momentum k can thus be chosen to lie in the Brillouin zone of the "even" sublattice $z_A=2z$. This zone is half the linear size of the zone of the full lattice, as shown in Fig. 11, and contains $N_s/4$ k points, for a lattice of N_s sites. Therefore, the set

$$\{|k,\Delta_1,\alpha\rangle,\ |k,\Delta_2,\alpha\rangle\}\ , \tag{9.12}$$

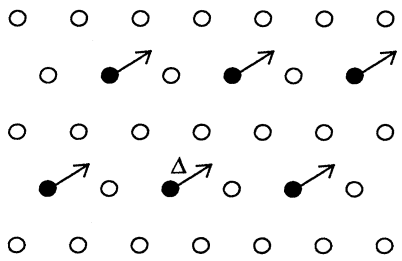

FIG. 10. Locations of Gaussian spinon orbitals superposed in the itinerant state (9.6). The arrows denote the displacement vector Δ.

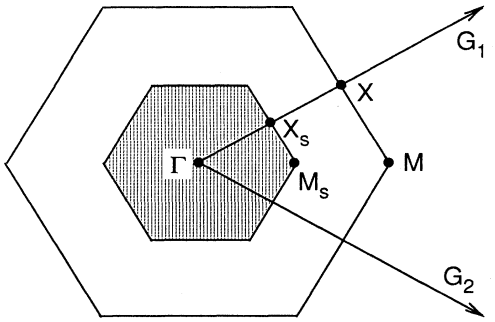

FIG. 11. Brillouin zone of the sublattice $z_A = 2z$ (shaded), and of the full direct lattice (outer contour). $\mathbf{G}_1$ and $\mathbf{G}_2$ are the generators of the reciprocal lattice.

where k is in the "small" Brillouin zone in Fig. 11, $\Delta_1 = 0$ and $\Delta_2 = b$ span the two-dimensional subspace ($k, \alpha = \text{const}$), and $\alpha = \uparrow, \downarrow$ is a spin label, is a complete basis of itinerant spinon states. The number of independent states with a given polarization is thus equal to $N_s/2$, half the number of lattice sites. This proves that the basis (9.1) with z_0 ranging over all sites is twice overcomplete.

The folding of the Brillouin zone and the twofold degeneracy of crystal momentum eigenstates are precisely what one expects[20] for a change-$e/2$ particle moving on the lattice in a background magnetic field with one-half of a flux quantum $2hc/e$ per unit cell. Our description of itinerant spinons is consistent with the picture of the frustrated antiferromagnet as a lattice gas of charge-e bosons, where a spinon is a quasiparticle of charge $e/2$.

The amount of dispersion in the spinon energy bands can be estimated from the overlaps of the localized orbitals (9.1). We consider the state in which a spinon localized on size z_A hybridizes with a near-neighbor orbital z'_A:

$$|\psi_{\text{hybrid}}, \downarrow\rangle = |z_A, \downarrow\rangle + e^{i\theta}|z'_A, \downarrow\rangle \ , \tag{9.13}$$

and compare the energy of this state with the total energy of a localized spinon, $E_{\text{on-site}}$. The energy gained by hybridization is

$$E_{\text{on-site}} - E_{\text{hybrid}}(\theta) = \frac{-t\cos\theta}{1 + f\cos\theta} \ , \tag{9.14}$$

where t and f are the near-neighbor energy and wave function overlaps defined by

$$t = \frac{\langle z'_A, \downarrow|\mathcal{H}|z_A, \downarrow\rangle}{\langle z_A, \downarrow|z_A, \downarrow\rangle} - fE_{\text{on-site}} \ , \tag{9.15a}$$

$$f = \frac{\langle z'_A, \downarrow|z_A, \downarrow\rangle}{\langle z_A, \downarrow|z_A, \downarrow\rangle} \ . \tag{9.15b}$$

The overlaps t and f were obtained by a Monte Carlo calculation similar to the one used in Sec. VIII to determine the on-site spinon creation energy Δ_s. For the near-neighbor overlaps, we find

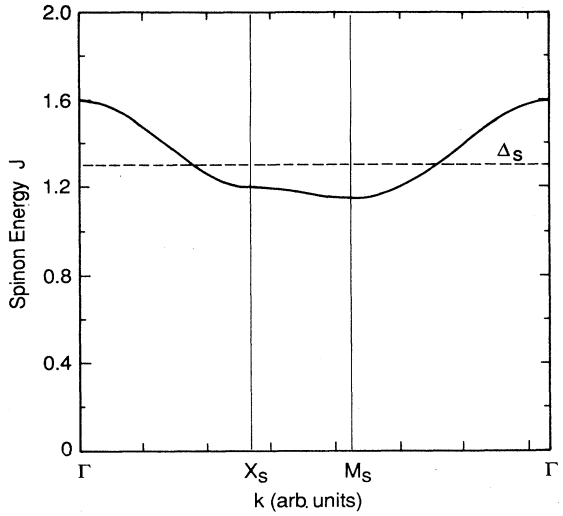

FIG. 12. Spinon energy band in the near-neighbor tight-binding approximation. The dashed line is drawn at the HNC value of Δ_s.

$$t/J = 0.042 \pm 0.024 \ ,$$

and

$$f = 0.389 \pm 0.005 \ .$$

The range of the hybridization energy (9.14) as a function of the phase angle θ is then 0.098 J, an order of magnitude smaller than the excitation energy $\Delta_s = 1.3J$ for a localized spinon.

Since spinons behave as charge-$e/2$ particles moving in a background magnetic field, a tight-binding approximation for the spinon energy band should look qualitatively similar to the dispersion of a charge-e boson, with three modifications. First, the size of the Brillouin zone is reduced in half, reflecting the fractional "charge" of the spinon; second, the bandwidth must be adjusted by the ratio of the spinon and boson hybridization energies; finally, a positive self energy Δ_s must be added. The shape of the resulting doubly degenerate spinon energy band is shown in Fig. 12. Since the energy overlap t is positive, the band disperses down from the zone center and reaches a minimum at the zone corner (point M_s in Fig. 11). In spite of the large error bars on the bandwidth, we expect the spinon excitation energy to remain positive everywhere in the Brillouin zone.

X. COLLECTIVE EXCITATIONS AND STABILITY OF THE SPIN LIQUID STATE

In view of the existence of competitive ordered variational wave functions[4] for the Heisenberg model on the triangular lattice, we address the question of stability of the spin liquid phase against crystallization, or antiferromagnetic long-range order. At sufficiently low densities, the two-dimensional electron gas in a magnetic field undergoes a phase transition from the fractional quantum Hall liquid state to a Wigner crystal. Crystallization occurs as a result of critical softening of a collective

mode[8] which becomes macroscopically occupied at the transition point, in a manner analogous to superfluid condensation in helium. This scenario is supported by the numerical results of Girvin *et al.*[11] which indicate that, as the electron density is reduced, the collective mode energy gap decreases, and its minimum as a function of q occurs close to the reciprocal lattice vector for a Wigner crystal.

Following Ref. 11, we use the variational ansatz

$$|q\rangle = S_q^\mu |\Psi\rangle \tag{10.1}$$

to describe the spin-1 collective excitations of the triangular lattice antiferromagnet. The operator S_q^μ is the Fourier component of the spin density,

$$S_q^\mu = \frac{1}{\sqrt{N_s}} \sum_{j=1}^{N_s} S_j^\mu e^{i\mathbf{q}\cdot\mathbf{r}_j}, \quad \mu = x,y,z \ , \tag{10.2}$$

and $|\Psi\rangle$ is the spin liquid state (3.1). Since both $|\Psi\rangle$ and the Hamiltonian are rotationally invariant, the modes generated by the operators S_q^x, S_q^y, and S_q^z are degenerate. When q is close to the critical wave vector q_c located in the corner of the full Brillouin zone (point M in Fig. 11), S_q^μ has a nonzero expectation value in a three-sublattice Néel state. We expect Néel ordering to be caused by macroscopic occupation of a mode with wave vector q_c, as its energy vanishes.

The expectation energy of the collective mode S_q^z is given by the Feynman-Bijl formula[11]:

$$\Delta(\mathbf{q}) = \frac{1}{2} \frac{\langle\Psi|[S^z_{-q},[\mathcal{H},S^z_q]]|\Psi\rangle}{S(q)} \ , \tag{10.3}$$

provided $|\Psi\rangle$ is the exact ground state of $\mathcal{H}$. Since we approximate the true ground state by (3.1), expression (10.3) can lead to an error of either sign in $\Delta(q)$. The static structure factor $S(q) = \langle\Psi|S^z_{-q}S^z_q|\Psi\rangle$ is related to the ground-state radial distribution function $g(r)$ (cf. Sec. III) as follows:

$$S(q) = \sum_{j=1}^{N_s} \{\tfrac{1}{4}[g(r_j)-1] + \tfrac{1}{2}\delta_{r_j,0}\} e^{i\mathbf{q}\cdot\mathbf{r}_j} \ . \tag{10.4}$$

Evaluation of the matrix element in the numerator of Eq. (10.3) yields

$$\langle\Psi|[S^z_{-q},[\mathcal{H},S^z_q]]|\Psi\rangle = -2J\chi(b|0) \sum_{n=1}^{6} (1-e^{i\mathbf{q}\cdot\boldsymbol{\delta}_n}) \ , \tag{10.5}$$

where

$$\chi(b|0) = \langle\Psi|S^+_{\mathbf{r}+\boldsymbol{\delta}_n} S^-_{\mathbf{r}}|\Psi\rangle$$

is the near-neighbor value of the ground-state density matrix and $\boldsymbol{\delta}_n$ are the vectors from a site to its near neighbors. Rotational symmetry of the ground state leads to the relation

$$\chi(b|0) = \tfrac{1}{2}[g(b)-1]$$

(see Eq. (6.2). All parameters in $\Delta(\mathbf{q})$ are thus contained in the ground-state radial distribution function.

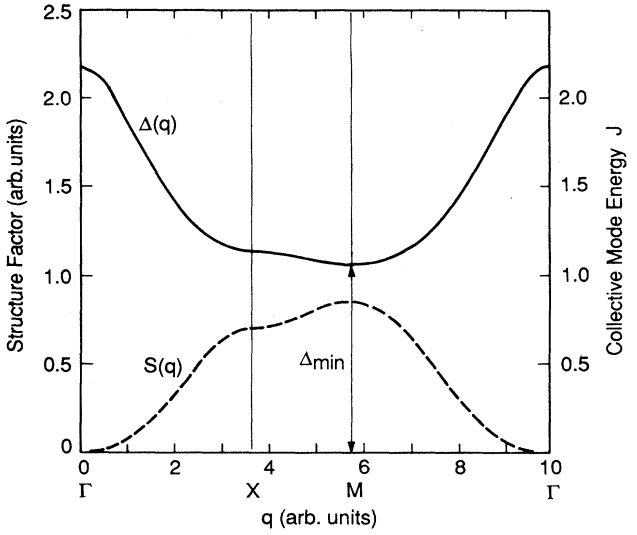

FIG. 13. Dashed line: static structure factor for the ground state (3.1); solid line: energy of the collective mode (10.1) along symmetry directions in the zone.

The static structure factor $S(\mathbf{q})$ and the collective mode energy $\Delta(\mathbf{q})$ on the triangular lattice are shown in Fig. 13. The minimum of $\Delta(\mathbf{q})$ at the critical wave vector $\mathbf{q}_c$ corresponding to three-sublattice Néel order is a direct effect of the peak in $S(\mathbf{q})$ at the same $\mathbf{q}$. Because of the moderate strength of this peak, our estimate of the collective mode energy gap is rather large: $\Delta_{\min} = 1.1J$. One expects the actual energy gap at $\mathbf{q}_c$ to be lower, since Néel-ordered states with energy close to the ground-state value have been shown to exist.[4] The large magnitude of the gap $\Delta_{\min}$ is likely to be related to an underestimate of the peak in the correct $S(q)$ by the variational ground state $|\Psi\rangle$. A single-mode approximation for the energy gap of a spin-1 Heisenberg chain, based on an approximate Jastrow ground state for this model,[21] exceeds the numerically determined zone-edge gap by a factor of 2, while yielding a tight upper bound on the gap of the extended Heisenberg model,[21,22] for which the Jastrow ground state is exact. More work is necessary to obtain a reliable estimate of the energy gap in the 2D antiferromagnet.

XI. STATISTICS OF SPINON EXCITATIONS

The statistics of spinons has recently been the subject of some debate.[12,23,24] On the other hand, there is considerable evidence that quasiparticle excitations in the quantum Hall system obey fractional statistics. Fractional statistics, originally discussed by Wilczek,[25] has been identified by Halperin[26] as the root cause of the hierarchy of fractional quantum Hall states.[27,18] It has also been shown to follow directly from the properties of the quasihole wave function.[28]

The physical content of the fractional statistics hypothesis in the quantum Hall system is in the collective behavior of fractionally charged quasiparticles at large

distances. Consider two identical quasiparticle excitations with charges νe, located at z_A and z_B and suppose the distance $|z_A - z_B|$ is large compared to the magnetic length. The two quasiparticles then behave as if they were charge-e bosons, each carrying a thin solenoid containing magnetic flux $\phi = \nu(hc/e)$ normal to the sample. Thus, if we treat excitations as bosons, the Hamiltonian for the quasiparticle at z_A must contain, in addition to Coulomb interactions and external fields, a long-range gauge coupling to the vector potential

$$\mathbf{A}(z_A, z_B) = \frac{\phi}{2\pi} \nabla_A [\arg(z_A - z_B)] , \tag{11.1}$$

produced by the solenoid attached to the quasiparticle at z_B.

In the continuum problem, the presence of the vector potential (11.1) can be detected by measuring the Berry phase acquired by the wave function of the two-quasiparticle system as quasiparticle A is adiabatically transported around a loop enclosing B. If the quasiparticles are boson-flux tube composites, the Berry phase contains two contributions: an Aharonov-Bohm phase due to the external magnetic flux through the loop, and a statistical phase generated by the flux tube attached to B. For quasiparticles with charge νe, the statistical part of the Berry phase is given by

$$\gamma_{\text{stat}}(C) = \frac{2\pi}{\phi_0} \oint_c \mathbf{A}(z_A, z_B) \cdot d\mathbf{l} = 2\pi\nu , \tag{11.2}$$

where c is the closed trajectory of quasiparticle A. Calculations of Arovas, Schrieffer, and Wilczek[29] have shown that the Berry phase for the quasihole excitation in the quantum Hall system contains a statistical contribution given exactly by (11.2).

The results of a similar Berry phase experiment on the lattice are difficult to interpret since the excitations then have energy dispersion, which introduces additional phases to the time-dependent wave function as the localized quasiparticle moves across the unit cell. We note, however, that the statistics of excitations of a lattice system can be determined from other quantities which are sensitive to the presence of the vector potential (11.1), e.g., from the hopping matrix elements between localized excited states, as discussed below.

It has been suggested[12] that spin-$\frac{1}{2}$ excitations of the RVB liquid state interact by the vector potential (11.1) with the fraction $\nu = \frac{1}{2}$. Disputing this claim, Kivelson and Rohksar[30] have argued that in a time-reversal-invariant system where the ground state and excitations are nondegenerate, only bose or fermi statistics are possible, and that spinons behave as fermions with no long-range forces. The key premise in this argument, the nondegeneracy of the eigenstates, is an assumption which has not been demonstrated to hold for the spin liquid state. It certainly does not hold for the variational spinon wave functions (7.1)–(7.4), since the time reverse of the state $\Psi_A^{\uparrow}$ is $\Psi_A^{\downarrow *}$, which is distinct from $\Psi_A^{\downarrow}$. Insofar as these wave functions provide a correct description of the spinon, numerical evidence indicates that there exists a spin-dependent gauge interaction between spinons, mediated by the vector potential

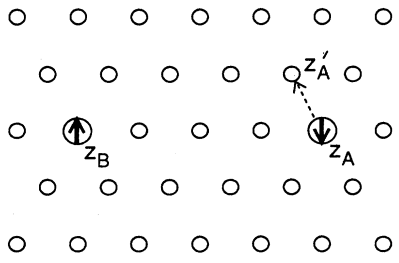

FIG. 14. Initial configuration of the quasihole (↓-spinon) and the quasiparticle (↑-spinon) in the calculation of the off-diagonal matrix elements between states (11.4).

$$\mathbf{A}(z_A, \sigma_A; z_B, \sigma_B) = \frac{1}{2} \frac{\phi_0}{2\pi} \nabla_A [\arg(z_A - z_B)] \boldsymbol{\sigma}_A \cdot \boldsymbol{\sigma}_B , \tag{11.3}$$

where $1/2\boldsymbol{\sigma}_A$ and $1/2\boldsymbol{\sigma}_B$ are the spins of the two particles. The phase generated by the vector potential (11.3) during the motion of two spinons changes sign depending on their relative polarization state. For two identical excitations, this gauge interaction is expected[28] to follow from the quasihole wave function (7.1) and (7.2). Our results for the quasihole-quasiparticle pair suggest an extension of the fractional statistics for spin-$\frac{1}{2}$ particles, given by (11.3).

Evidence for the gauge interaction (11.3) comes from numerical calculations of the off-diagonal overlap matrix elements between two-spinon states. Consider a quasihole localized at z_A and a quasiparticle at z_B, and suppose the quasihole hops from z_A to $z_{A'}$, as shown in Fig. 14. In the boson representation, the initial state is described by

$$|z_A \downarrow, z_B, \uparrow\rangle = e^{(-1/8)(|z_A|^2 + |z_B|^2)} S^{\downarrow}_{z_A} S^{\uparrow}_{z_B} |\Psi\rangle , \tag{11.4}$$

which is symmetric under interchange of $(z_A, \downarrow)$ and $(z_B, \uparrow)$, since the operators $S^{\downarrow}_{z_A}$ and $S^{\uparrow}_{z_B}$ defined by (7.2) and (7.4) commute. The matrix elements of the overlap $\langle z'_A \downarrow, z_B \uparrow | z_A \downarrow, z_B \uparrow \rangle$ in the this representation have been evaluated by the Monte Carlo method. The phases of these matrix elements for near-neighbor hops $z_A \rightarrow z'_A$ are

TABLE IV. Phases of the matrix elements $\langle z'_A \downarrow, z_B \uparrow | z_A \downarrow, z_B \uparrow \rangle$ in the representation (11.4) for each of the six near-neighbor hops $z_A \rightarrow z'_A$. The initial state is $z_A = 2b$, $z_B = -2b$, and the units are radians.

z'_A/b	Monte Carlo	Eq. (11.5)
3	-0.0008	0.0000
$(5+i\sqrt{3})/2$	$-0.9994+\pi$	$-0.0951+\pi$
$(3+i\sqrt{3})/2$	$-0.1241+\pi$	$-0.1213+\pi$
1	-0.0001	0.0000
$(3-i\sqrt{3})/2$	$0.1056+\pi$	$0.1213+\pi$
$(5-i\sqrt{3})/2$	$0.0947+\pi$	$0.0951+\pi$

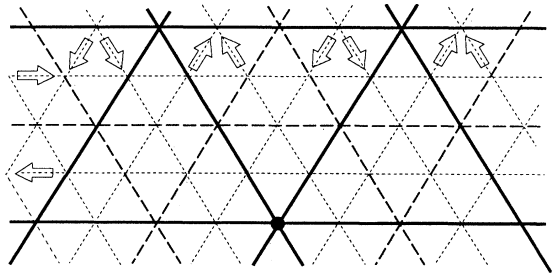

FIG. 15. Aharonov-Bohm phases $f_b = e^{i\gamma_b}$ in the hopping matrix elements of a quasihole. Solid lines, $f_b = 1$; dashed lines, $f_b = -1$; dotted lines, $f_b = i$ in the direction of the arrows. The circle denotes the origin.

compared in Table IV with the phases generated by the total vector potential **A** acting on the quasihole. We assume the **A** consists of the statistical term (11.3) and the contribution (2.4) which describes the uniform background frustration flux. The total phase change is then obtained as follows:

$$\gamma(z'_A, z_A) = \gamma_b - \tfrac{1}{2}\arg\left[\frac{z'_A - z_B}{z_A - z_B}\right] . \tag{11.5}$$

The background Aharonov-Bohm phase factors $e^{i\gamma_b}$ for all near-neighbor hops of a charge-$\frac{1}{2}$ quasihole are shown in Fig. 15. We note that the off-diagonal matrix elements of the Hamiltonian $\mathcal{H}$ must behave in the same manner as functions of z_A, z'_A, and z_B since $\mathcal{H}$ acts only on the individual spin degrees of freedom. The spinons, as represented by Eqs. (7.1)–(7.4), can thus be thought of as charged bosons moving in a uniform magnetic field and interacting via the vector potential (11.3). This implies that the natural wave function representation for the spinons is the fractional statistics representation,[8,28] in which long-range gauge interactions disappear from the effective spinon Hamiltonian.

XII. SUMMARY AND CONCLUSIONS

We have presented a theory of the spin liquid state in a two-dimensional quantum antiferromagnet which draws on an analogy with the fractional quantum Hall effect system. The ground state of the theory is described variationally by the $m = 2$ quantum Hall wave function which is shown to be a liquid, by employing the analogy with the classical lattice plasma, and a spin singlet, by virtue of its analytic properties. The spin liquid state can be viewed as evolving from the ground state of the continuum quantum Hall Hamiltonian for bosons, as the lattice perturbation is turned on adiabatically, transforming the system into a lattice gas representation of the antiferromagnet. If the quantum Hall energy gap remains finite in this process, which we believe to be the case, the theory predicts the existence of spin-$\frac{1}{2}$ neutral excitations (spinons). These appear as the magnetic analogues of the fractionally charged quantum Hall quasiparticles. We describe the two polarization states of a spinon by the quantum Hall quasihole wave function and its spin inverse. This representation is shown to behave as a spin-$\frac{1}{2}$ doublet under rotations and to yield a finite excitation energy for the spinon states, supporting the idea that the excitation spectrum of the system has an energy gap. A single mode approximation for the collective mode energy also gives a finite, though probably overestimated, value for the gap. Finally, the structure of the overlaps of spinon states in the quantum Hall wave function representation shows that these wave functions describe spin-$\frac{1}{2}$ particles with fractional $\frac{1}{2}$ statistics.

These results reveal a similarity between the fractional quantum Hall system and the two-dimensional antiferromagnets characterized by an RVB-type spin liquid ground state. There remains, however, the task of proving that such an incompressible spin liquid and its excitations exist as true eigenstates of a 2D spin-$\frac{1}{2}$ Hamiltonian. The low variational energy of the spin liquid state for the near-neighbor Heisenberg model on the triangular lattice and the short range of its spin correlations indicate that longer-range spin interactions, e.g., second-near-neighbor coupling, can push the system further into the liquid phase. Among questions deserving further attention is the lack of time reversal symmetry, a property of the spin liquid state which follows from the quantum Hall analogy, and its effect on the statistics of excitations in the RVB state.

ACKNOWLEDGMENTS

We thank F. D. M. Haldane, A. P. Young, S. A. Kivelson, D. Rokhsar, P. W. Anderson, and S. Doniach for helpful discussions. This work was supported primarily by the National Science Foundation under Grant No. DMR-85-10062 and by the National Science Foundation–Materials Research Laboratories (NSF-MRL) program through the Center for Materials Research at Stanford. Additional support was provided by the U.S. Department of Energy through the Lawrence Livermore National Laboratory under Contract No. W-7405-Eng-48.

[1] V. Kalmeyer and R. B. Laughlin, Phys. Rev. Lett. **59**, 2095 (1987).
[2] P. W. Anderson, Mater. Res. Bull. **8**, 153 (1973).
[3] P. W. Anderson, Science **235**, 1196 (1987).
[4] D. A. Huse and V. Elser, Phys. Rev. Lett. **60**, 2531 (1988).
[5] S. Liang, B. Doucot, and P. W. Anderson, Phys. Rev. Lett. **61**, 365 (1988).
[6] R. B. Laughlin, Ann. Phys. (N.Y.) **191**, 163 (1989).
[7] R. B. Laughlin, Phys. Rev. Lett. **50**, 1395 (1983).
[8] R. B. Laughlin, in *The Quantum Hall Effect*, edited by R. E. Prange and S. M. Girvin (Springer, New York, 1987), p. 233.
[9] P. W. Anderson, G. Baskaran, Z. Zou, and T. Hsu, Phys. Rev. Lett. **58**, 2790 (1987).
[10] S. A. Kivelson, D. S. Rokhsar, and J. P. Sethna, Phys. Rev. B

35, 8865 (1987).
[11]S. M. Girvin, A. H. MacDonald, and P. M. Platzman, Phys. Rev. B **33**, 2481 (1984).
[12]R. B. Laughlin, Science **242**, 525 (1988).
[13]L. D. Fadeev and L. A. Takhtajan, Phys. Lett. **85A**, 375 (1981).
[14]W. Marshall, Proc. R. Soc. (London) **A232**, 48 (1955).
[15]F. D. M. Haldane, Phys. Rev. Lett. **61**, 1029 (1988).
[16]H. Nishimori and H. Nakanishi, J. Phys. Soc. Jpn. **57**, 626 (1988).
[17]G. Stell, in *Equilibrium Theory of Classical Liquids,* edited by H. L. Frisch and J. L. Lebowitz (Benjamin, New York, 1964); L. E. Reichl, *A Modern Course in Statistical Physics* (University of Texas, Austin, 1980).
[18]A. Chang, in *The Quantum Hall Effect,* edited by R. E. Prange and S. M. Girvin (Springer, New York, 1987), p. 175.
[19]R. B. Laughlin, in *Two-Dimensional Systems, Heterostructures, and Superlattices,* edited by G. Bauer, F. Kuchar, and H. Heinrich (Springer, Berlin, 1984).
[20]E. Brown, in *Solid State Physics,* edited by F. Seitz, D. Turnbull, and H. Ehrenreich (Academic, New York, 1968), Vol. 22, p. 313.
[21]D. P. Arovas, A. Auerbach, and F. D. M. Haldane, Phys. Rev. Lett. **60**, 531 (1988).
[22]I. Affleck, T. Kennedy, E. H. Lieb, and H. Tasaki, Phys. Rev. Lett. **59**, 799 (1987).
[23]S. A. Kivelson, Phys. Rev. B **39**, 259 (1989).
[24]N. Read and B. Chakraborty (unpublished).
[25]F. Wilczek, Phys. Rev. Lett. **49**, 957 (1982).
[26]B. I. Halperin, Phys. Rev. Lett. **52**, 1583 (1984).
[27]F. D. M. Haldane, Phys. Rev. Lett. **51**, 605 (1983).
[28]R. B. Laughlin (unpublished).
[29]D. P. Arovas, J. R. Schrieffer, and F. Wilczek, Phys. Rev. Lett. **53**, 722 (1984).
[30]S. A. Kivelson and D. S. Rokhsar, Phys. Rev. Lett. **61**, 2630 (1988).